

Chapter 6

METABOLITE IDENTIFICATION BY LC-MS: APPLICATIONS IN DRUG DISCOVERY AND DEVELOPMENT

Cornelis E.C.A. Hop and Chandra Prakash

6.1. Introduction

Recent data indicate that the discovery and development of a new drug costs around 1 billion dollars and it may take approximately 10 years for the drug to reach the marketplace (Fig. 1). Considering these staggering numbers, it is critical that efforts are made to reduce attrition of drug candidates during the various stages of drug discovery and development. One of the sources of attrition can be inappropriate drug disposition characteristics. Indeed, data from a joint meeting from the Pharmaceutical Manufacturers Association (PMA) and the Food and Drug Administration (FDA) in 1991 showed that about 40% of all lead candidates failed in their development due to poor pharmacokinetics (Baillie and Pearson, 2000). Thus, it is critical that attention is paid to the disposition characteristics of a drug candidate early on. This information sheds light on the absorption, distribution, metabolism and excretion (ADME) of potential drugs (Lin and Lu, 1997; Borchardt *et al.*, 1998; Eddershaw and Dickins, 1999; Woolf, 1999; White, 2000; Riley *et al.*, 2002; Smith *et al.*, 2002) and these studies are performed (a) to support the selection of more efficacious and safer drugs for development, (b) to help understand pharmacological and toxicological observations and (c) to determine dose levels and dose regimens. Up to 1985, the disposition of a drug candidate was examined predominantly once the compound reached phase I or subsequent clinical trials. However, around 1990, most major drug companies started to explore the drug disposition characteristics of lead candidates during the discovery stage of drug development. The ADME data was being used to guide synthetic chemistry efforts in order to come up with candidates with more appropriate drug disposition characteristics. This approach appears to have been successful because informal data suggest that the attrition due to inappropriate ADME characteristics has been reduced significantly.

Currently, a wide variety of *in vitro* and *in vivo* screens are in place to obtain valuable information about ADME parameters for lead candidates. The *in vitro* studies include (a) metabolic stability in liver microsomes, hepatocytes or with recombinant cytochrome P450 enzymes, (b) metabolite formation in liver microsomes, hepatocytes

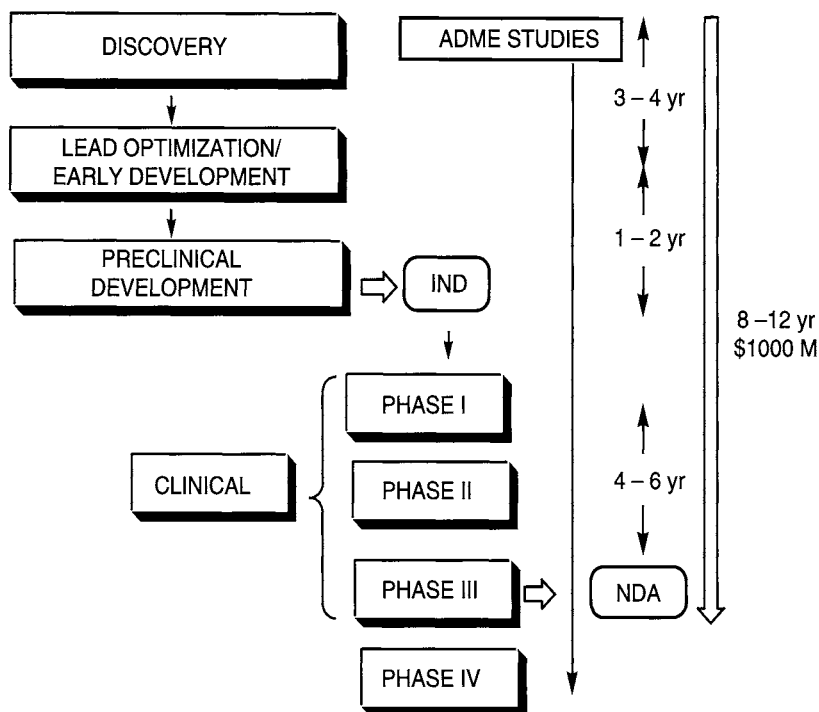


Figure 1.
Generic timeline for the various stages of drug discovery and development

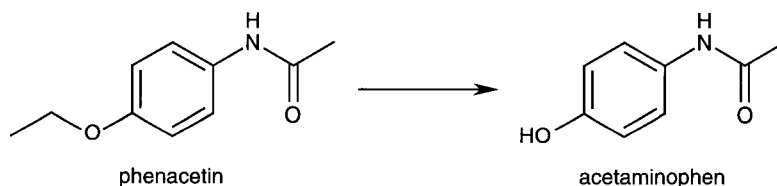
or with recombinant cytochrome P450 enzymes, (c) absorption/transport studies in Caco-2 cells or cell lines over expressing various transporters, (d) cytochrome P450 inhibition, (e) cytochrome P450 induction, (f) plasma protein binding and (g) red blood cell partitioning. The in vivo studies include (a) pharmacokinetic studies via various routes of administration (oral, intravenous, subcutaneous, etc.), (b) tissue distribution (e.g., brain penetration) and (c) metabolite identification in various biological fluids (plasma, bile, urine, etc.). It has been shown that many of these studies benefit from analysis by liquid chromatography interfaced with mass spectrometry (LC-MS) (Niessen, 1998; Willoughby *et al.*, 1998; Lee and Kerns, 1999; Lee, 2002).

In the recent past, analysis of biological samples was a bottleneck. In some cases GC-MS, with or without derivatization of the analyte, was possible, but in many cases more traditional analytical techniques were employed, such as radioimmunoassays or HPLC with UV, fluorescence or electrochemical detection. With the introduction of atmospheric pressure ionization (API), in particular electrospray ionization (ESI) and atmospheric pressure chemical ionization (APCI), in the late 1980s, it became possible to sample liquids directly by mass spectrometry. Shortly after the introduction of these ionization techniques, they were employed in combination with liquid chromatography for pharmacokinetic studies and metabolite identification. The availability of LC-MS

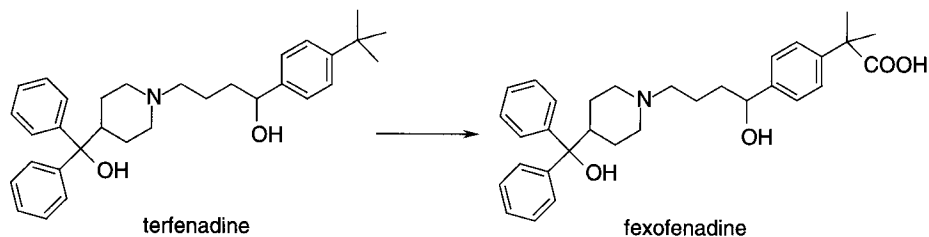
enabled increased and earlier ADME evaluation in drug discovery and development. With minimal effort, it became possible to develop sensitive and selective assays for drug candidates and, if required, their metabolites. Recent developments, such as monolithic columns, ballistic gradients and parallel analytical columns, have increased the throughput of LC-MS for quantitative *in vitro* and *in vivo* studies dramatically (Bakhtiar *et al.*, 2002; Cox *et al.*, 2002; Hopfgartner and Bourgoigne, 2003). Another area, which benefited greatly from the introduction of LC-MS, is metabolite identification. Both the general approach and specific examples displaying the power of LC-MS for metabolite identification will be presented here. For general reviews describing the use of LC-MS in drug disposition studies see Korfmacher *et al.* (1997), Poon (1997), Brewer and Henion (1998), Baillie and Pearson (2000) and Rossi and Sinz (2002).

6.2. Metabolite Identification

Drugs are metabolized generally to more polar, hydrophilic entities, which can be excreted from the body more easily. The main routes of elimination are bile and urine. Detailed knowledge of the metabolic fate of drugs is important because the metabolites could be (a) pharmacologically active, (b) toxic, (c) involved in drug-drug interactions via inhibition or induction of drug-metabolizing enzymes or (d) competing for plasma protein binding with the parent compound. Examples include phenacetin, which is metabolized to acetaminophen and the latter compound is responsible for the majority of the analgesic activity.

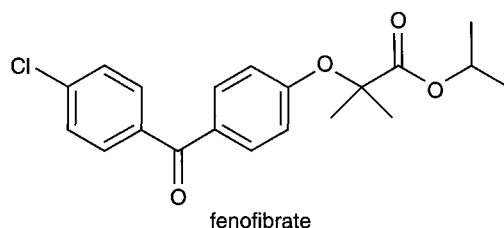


A few years ago, terfenadine was withdrawn from the market, because it is metabolized by CYP3A4 to fexofenadine and inhibition of its metabolism by CYP3A4 inhibitors, such as erythromycin and ketoconazole, can give rise to elevated levels of terfenadine, which can cause cardiotoxicity. However, the metabolite, fexofenadine, is marketed, because it does not have these interactions and is pharmacologically active.



During toxicology studies, detailed knowledge about the metabolism is important, because, for proper assessment of the safety of a drug for human use, it must be shown that the animal species used for safety evaluation are exposed to the same metabolites as humans. If this is not the case, specific toxicology studies with the metabolite(s) not formed in the animal species may be needed.

In the discovery stage, identification of metabolites may reveal metabolic liabilities in molecules, which can subsequently be addressed by medicinal chemists who can block these particular sites of metabolism. This could result in the discovery of drug candidates with superior pharmacokinetic properties. Alternatively extensive metabolism has been used to create prodrugs, which may be better absorbed than the drug itself (e.g., fenofibrate). Thus, details about the metabolism of a drug and the enzymes involved in the metabolism are a necessity throughout drug discovery and development.



6.3. Mass Spectrometers For Metabolite Identification

Although impressive metabolite identification data have been obtained with GC-MS, the convenience of interfacing conventional LC columns with atmospheric pressure ionization sources has shifted metabolite identification studies toward employing almost exclusively LC-MS. The two most commonly employed atmospheric pressure ionization techniques are APCI and ESI. In APCI, also called heated nebulizer, the effluent from the LC column is converted into a fine mist via nebulization caused by a high velocity jet of air or nitrogen. The spray travels through a quartz tube heater, which vaporizes the droplets and, consequently, the analyte in the gas stream. A corona discharge from a needle initiates chemical ionization using the vaporized solvent as the reagent gas. Approximately 5–10 kV is applied to the needle, which generates a 2–5 μ A corona discharge current. For the generation of positive ions, the needle is at a high positive voltage with respect to counter electrode. A high negative voltage is used for the production of negative ions.

In ESI a dilute solution is sprayed from a fine needle, which carries a high potential (about 3–5 kV). If the needle carries a positive potential, the droplets will have an excess of positive charges, usually protons. Evaporation of the volatile solvent (e.g., H₂O, CH₃OH or CH₃CN) results in increased Coulombic repulsion between the positive charges, which eventually results in fragmentation of the droplet, generating smaller droplets. There are two theories for ion formation in ESI. Iribane and Thomson have suggested that ionized sample molecules are expelled from the droplets. Alternatively, it has been proposed that single, ionized sample molecules

remain after continuous solvent evaporation and droplet fragmentation. One of characteristic features of ESI is the mild nature of the ionization process, which usually results in the formation of $[M + H]^+$ or $[M - H]^-$ ions only. The absence of fragment ions necessitates MS/MS experiments to obtain structural information (*vide infra*).

A wide range of mass spectrometers has been used for metabolite identification and several new types have become available recently. The most frequently used instruments are single and triple quadrupole and 3-dimensional ion trap mass spectrometers. Time-of-flight, quadrupole-time-of-flight (Q-TOF), linear ion trap and Fourier-transform mass spectrometers have been used as well. In many ways, the instruments listed above are complementary. Although detailed descriptions of these types of mass spectrometers have been presented elsewhere, it is important to describe specific advantages and disadvantages of these types of mass spectrometers for metabolite identification.

6.3.1. Single and Triple Quadrupole Mass Spectrometer

With single and triple quadrupole mass spectrometers, MS data can be obtained by scanning the first quadrupole and detecting the mass-separated ions. Product ion MS/MS data can be obtained with a triple quadrupole mass spectrometer by mass-selecting the ions of interest with the first quadrupole, fragmenting these ions in the collision cell and mass separating the ions with the third quadrupole for subsequent detection. Triple quadrupole mass spectrometers also allow constant neutral loss and precursor ion MS/MS experiments. A constant neutral loss scan allows detection of all ionized compounds, which lose a specific entity upon collision-induced dissociation. For example, sulfate-conjugated metabolites are known to lose SO_3 (i.e., 80 Da) easily upon collision-induced dissociation and, therefore, an 80 Da constant neutral loss allows detection of all sulfate-conjugated metabolites present in the sample of interest. Precursor ion scans allow detection of all ionized compounds, which give rise to a specific fragment ion upon collision-induced dissociation. For example, glucuronide-conjugated metabolites frequently yield a signal at m/z 175 in the negative ion mode and this "fingerprint" can be used to detect glucuronide-conjugated metabolites. Constant neutral loss and precursor ion scans greatly facilitate the process of finding metabolites, especially if the matrix contains many endogenous components. The various MS/MS scan modes available for a triple quadrupole mass spectrometer are summarized in Fig. 2 and the availability of multiple MS/MS scan modes increases the selectivity of this type of mass spectrometers significantly. Finally, triple quadrupole mass spectrometers can operate in the selected reaction-monitoring (SRM) mode. In this mode, a specific ion is mass-selected with the first quadrupole and fragmented in the collision cell and the third quadrupole is set to transmit a specific fragment ion. This mode results in greatly enhanced sensitivity compared to full scan MS/MS experiments.

6.3.2. 3-Dimensional Ion Trap Mass Spectrometer

In a 3-dimensional ion trap mass spectrometer all ions are in the center of the ion trap and a spectrum is obtained by sequentially ejecting ions out of the trap. For

ionization		fragmentation		detection	
ABC ⁺	→	A ⁺ + BC → AB + C ⁺ →		A ⁺ C ⁺	product ion spectrum
ABD ⁺	→	A ⁺ + BD → AB + D ⁺ →		A ⁺ D ⁺	
ABC ⁺	→	A ⁺ + BC → AB + C ⁺ →		A ⁺	precursor ion spectrum
ABD ⁺	→	A ⁺ + BD → AB + D ⁺ →		A ⁺	
ABC ⁺	→	A ⁺ + BC → AB + C ⁺ →		C ⁺	constant neutral loss spectrum
ABD ⁺	→	A ⁺ + BD → AB + D ⁺ →		D ⁺	

Figure 2.

Scan modes feasible with a triple quadrupole mass spectrometer

a product ion MS/MS spectrum, the ions with a lower and higher molecular weight than that of the desired ions are ejected and the remaining ions with the desired m/z value are activated, which results in fragmentation. Because of the 3-dimensional nature of the ion trap, MS^n is possible and this can provide more information about the structure of a metabolite. (In the ion trap, MS/MS and MS^n are performed in “time” rather than in “space” as is the case for a triple quadrupole mass spectrometer.) However, constant neutral loss and precursor ion MS/MS data cannot be obtained with an ion trap mass spectrometer. For more details about the use of a 3-dimensional ion trap for metabolite identification see Tiller *et al.* (1998) and Dear *et al.* (1999).

6.3.3. Q-TOF Mass Spectrometer

The Q-TOF mass spectrometer was introduced in 1996 and has found widespread use for metabolite identification. In the MS mode the time-of-flight analyzer is used for mass analysis. For product ion MS/MS spectra, the ions of interested are selected with the first quadrupole and the fragment ions are mass-separated with the time-of-flight analyzer. The advantages of the Q-TOF mass spectrometer are sensitivity, scan speed and mass accuracy. The mass accuracy is usually within 5 ppm and, therefore, it is possible to assign a specific molecular formula to the

metabolite under investigation (Hopfgartner *et al.*, 1999; Hop *et al.*, 2001; Qin and Frech, 2001; Tiller *et al.*, 2001).

Thus, each type of mass spectrometers has specific strengths and frequently more than one type is used to come up with more definitive structural data for metabolites.

6.3.4. Common Biotransformations

Subsequent to acquisition, MS spectra can be inspected for the presence of (anticipated) phase I metabolites. Table 1 presents a list of common phase I biotransformations and the corresponding mass changes. The most common metabolic process is oxidation resulting in a hydroxy moiety, which generates an $M + 16$ Da metabolite. Liver microsomes are frequently used to assess formation of phase I metabolites by a compound. Most phase I biotransformations are mediated by the ubiquitous cytochrome P450 enzymes. Table 2 presents a list of common phase II biotransformations and the

Table 1.

Common phase I biotransformations and the corresponding change in mass of the parent compound

Mass change (Da)	Type of biotransformation
-28	Deethylation ($-C_2H_4$)
-14	Demethylation ($-CH_2$)
-2	Two-electron oxidation ($-H_2$)
+2	Two-electron reduction ($+H_2$)
+14	Addition of oxygen and two-electron oxidation ($+O-H_2$)
+16	Addition of oxygen ($+O$)
+18	Hydration ($+H_2O$)
+30	Addition of two oxygen atoms and two-electron oxidation ($+2O-H_2$)
+32	Addition of two oxygen atoms ($+2O$)

Table 2.

Common phase II conjugation reactions and the corresponding change in mass of the parent compound

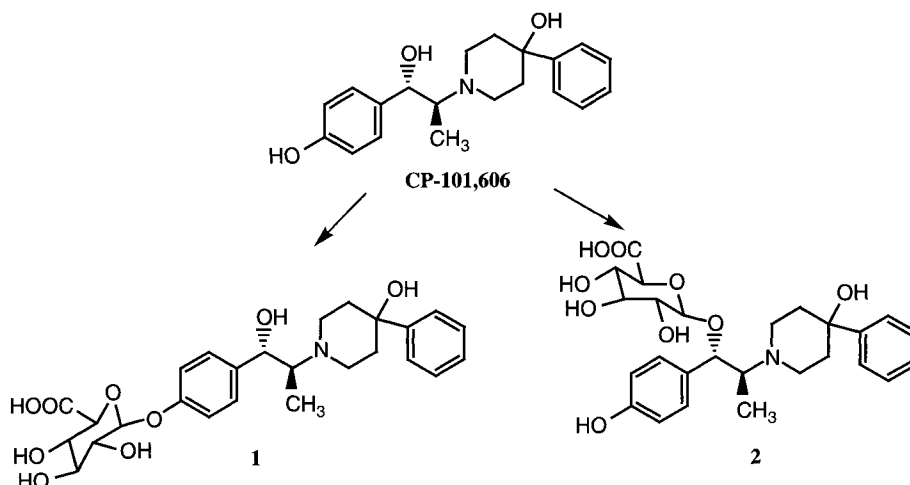
Mass change (Da)	Conjugate
+42	Acetyl
+80	Sulfate
+57	Glycine
+107	Taurine
+176	Glucuronide
+307 or 305	Glutathione

corresponding mass changes. Phase II biotransformations involve conjugation of the compound, with the objective of making the drug more hydrophilic. These phase II biotransformations are mediated by enzymes, such as *N*-acetyl transferases, sulfotransferases, UDP glucuronosyltransferases and glutathione-S-transferases. Both phase I and phase II enzymes are present in hepatocytes. Although MS data are frequently sufficient to identify the type of biotransformation taking place, product ion MS/MS spectra are necessary to identify the location of the structural modification. Interpretation of MS/MS data is time-consuming and requires a high level of expertise. (Several textbooks are available discussing interpretation of MS/MS data in detail.) Reliable software to automate interpretation of product ion MS/MS spectra is not yet available.

6.4. Additional Tools For Metabolite Identification

6.4.1. Chemical Derivatization

Although product ion MS/MS data can provide a substantial amount of structural information for metabolite identification, it is sometimes difficult to differentiate between regioisomers. For example, based on the product ion MS/MS spectra alone, it was not possible to define the site of glucuronidation for two glucuronide conjugates, **1** and **2**, of CP-101,606 (an NMDA receptor antagonist) observed in humans (Johnson *et al.*, 2003). The site of conjugation was established after derivatization of the sample with diazomethane. After treatment of **1** with diazomethane, the full-scan MS spectrum showed an intense protonated molecule at m/z 518, 14 Da higher than **1**, suggesting that the phenolic group was substituted with glucuronide. On the other, the full-scan MS spectrum of the methylated product of **2** showed an intense protonated molecule at m/z 532, 28 Da higher than **2**, indicating the methylation of both phenolic group as well as the carboxylic acid moiety of the glucuronide and, therefore, **2** was characterized as a benzylic glucuronide.



A few common derivatization reactions are presented in Table 3 and others can be found in the literature (Knapp, 1979). Sometimes derivatization of a metabolite is employed to create a more hydrophobic, readily ionizable entity. Dalvie *et al.* (1998) dansylated several polar urinary metabolites of a proprietary compound, which were detectable by radiochromatography, but which could not be identified by LC-MS. The presence of the dimethylamino group in the dansyl moiety facilitated protonation and characterization of the metabolites by LC-MS. An additional advantage is that increasing the molecular weight of the analyte frequently reduces the amount of chemical interference.

6.4.2. Radiolabeled Compounds

During the later stages of drug discovery or drug development a radiolabeled (^3H and/or ^{14}C) analog is synthesized to obtain more detailed metabolism and disposition data. In vitro studies can be performed using the radiolabeled analog. Upon LC-MS analysis the column eluent is split with a fraction going to the mass spectrometer for detection and the remainder going to an on-line radio-flow detector or a fraction collector for offline liquid scintillation counting (LSC). The radiochromatogram provides the retention times of all metabolites generated (unless the radiolabel is not retained in the metabolite) and, therefore, the inspection of mass spectrometric data for identification of metabolites can be more focused. Only a narrow region of the total-ion-current (TIC) trace, as specified by the radiochromatogram, needs to be examined for drug-related components. A small amount of a radiolabeled compound can be administered to animals or humans as well. LSC of the various biological fluids (usually plasma, bile and urine) helps identify the fluid with the largest amount of radioactivity and this fluid can be subsequently examined by LC-MS for identification of metabolites.

6.4.3. Isotope Patterns

If the parent compounds contains a characteristic (stable) isotope pattern, for example, due to the presence of one or more chlorine or bromine atoms, the metabolites can be identified by looking for this specific isotope pattern (cluster analysis).

Table 3.

Common reagents used to derivatize compounds

Reagent	Derivatization reaction
Anhydrous methanolic HCl	Methylation of carboxylic acids and allylic and benzylic alcohols
LiAlH_4 or NaBH_4	Reduction of aldehydes to alcohols
TiCl_3	Reduction of <i>N</i> -oxides
Acetic anhydride	Acetylation of amines and phenols

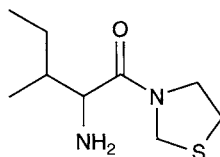
The presence of the desired isotope pattern increases the confidence that the signal is indeed related to the administered compound. Wienkers *et al.* (1995, 1996) identified metabolites for tirilazad, a potent inhibitor of membrane lipid peroxidation, and they employed a mixture of unlabeled and [2,4,6-¹³C₃, 1,3-¹⁵N₂-pyrimidine]tirilazad; metabolites were identified by looking for two signals of equal abundance separated by 5 Da.

6.4.4. LC–NMR–MS

Although LC–MS is a sensitive analytical technique for obtaining molecular weights and molecular formulas for metabolites, it provides only limited structural information. Due to the nature of the fragmentation pattern in product ion MS/MS spectra it is only possible to identify the moiety where structural modification has occurred without being able to isolate the specific site. If an authentic standard is available, a comparison of the HPLC retention times, as well as MS and MS/MS spectra may be sufficient to make more definitive assignments. Nuclear magnetic resonance (NMR) spectroscopy is frequently required to obtain the exact structure of each metabolite. The NMR spectrum can be obtained following isolation of the metabolite of interest. Alternatively, LC–NMR–MS can be employed (Shockcor *et al.*, 1996; Burton *et al.*, 1997; Clayton *et al.*, 1998; Loudon *et al.*, 2000). In the latter case, about 95% of the LC eluent is directed into the NMR spectrometer and the remainder is diverted into the mass spectrometer. Several elegant applications have appeared, especially in combination with generation of metabolites in bioreactors, but NMR spectroscopy still suffers from limited sensitivity compared to mass spectrometry, which makes this technique less practical for the identification of minor metabolites.

6.4.5. H/D Exchange

Frequently, the use of D₂O as the mobile phase for HPLC can be as informative as derivatization procedures. The number of exchangeable hydrogen atoms can provide valuable information about the functional groups present in the analyte. For example, it was feasible to distinguish two possible structures for an oxidative metabolite of a drug candidate containing a thiazolidine moiety (Liu *et al.*, 2001). If hydroxylation of one of the carbon atoms of the thiazolidine group occurred, the H/D shift should be one more than anticipated for the sulfoxide. H/D exchange also facilitates distinguishing *N*-oxides from hydroxylated metabolites. Other examples have been presented by Olsen *et al.* (2000).



6.5. Applications

Several examples are presented illustrating the use of various types of mass spectrometers to facilitate metabolite identification. It is critical to realize that, although LC-MS is a very powerful and useful technique, definitive assignments frequently require the use of additional analytical techniques (such as NMR) and/or the synthesis of authentic standards.

6.5.1. Metabolism of a Potent Neurokinin 1 Receptor Antagonist

Substance P is the most abundant neurokinin in the human central nervous system. The substance P preferring neurokinin-1 (NK1) receptor is highly expressed in brain regions that are critical for regulation of neurochemical responses to stress. NK1 receptor antagonists have been proven in concept to have excellent potential for the treatment of major depression (Kramer *et al.*, 1998) and their side effect profile might allow favorable differentiation against currently available therapies. In addition, NK1 receptor antagonists allow superior and sustained protection from acute and delayed chemotherapy-induced emesis (Navari *et al.*, 1999; Tattersall *et al.*, 2000). Here, the metabolism of a potent NK1 receptor antagonist, [3R,5R,6S]-3-(2-cyclopropyloxy-5-trifluoromethoxyphenyl)-6-phenyl-1-oxa-7-azaspiro[4.5]decane, (compound A hereafter; see Fig. 3) in rat plasma as well as in rat liver microsomes and rat hepatocytes is described (Hop *et al.*, 2002).

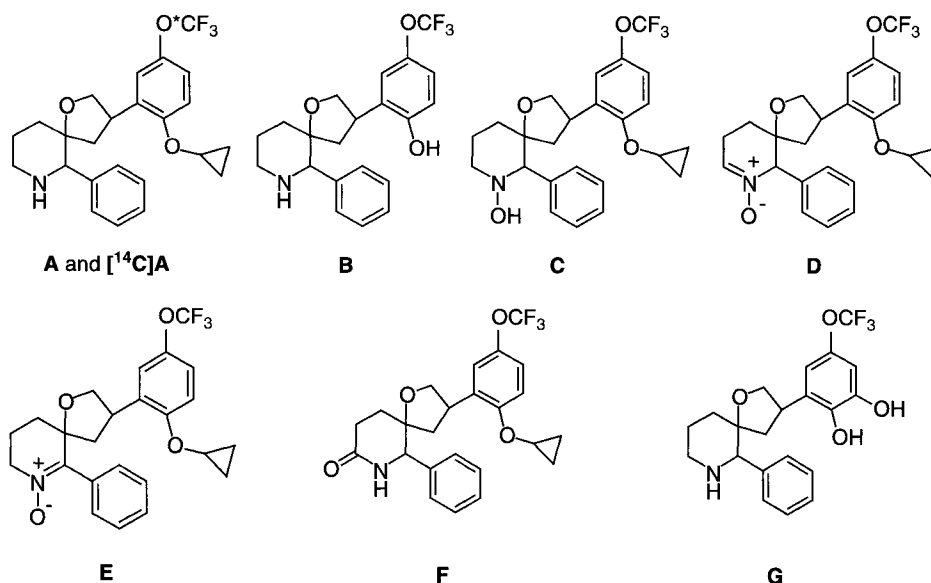


Figure 3.

Structures of compound A and its metabolites (* indicates the position of the ¹⁴C-label)

Interpretation of product ion spectra of metabolites frequently hinges upon similarity with that of the parent compound. However, sometimes interpretation of the product ion spectrum of the parent compound is ambiguous. Availability of ^{14}C -labeled compound **A** with the label in the trifluoromethyl group facilitated interpretation of the product ion spectrum. Comparison of the product ion spectrum of compound **A** with that of its ^{14}C -labeled analog indicates that the fragments at m/z 231, 215, 203, 191 and 175 are associated with the trifluoromethoxy phenyl moiety, whereas the fragments at m/z 184, 172, 159, 131, 91 and 56 are associated with the phenyl piperidine moiety. Accurate mass measurements obtained with a Q-TOF mass spectrometer provided additional information. Table 4 summarizes the molecular formula assignments for the major fragment ions of $[\text{A} + \text{H}]^+$; all assignments are within 10 ppm with most of them being within 5 ppm. Based on this information, structural assignments for the most informative fragmentation pathways of $[\text{A} + \text{H}]^+$ ions are feasible and the data are summarized in Fig. 4. Concern about the potential pharmacological activity of anticipated metabolites led to synthesis of authentic standards of the *O*-dealkylated metabolite (**B**), the hydroxylamine metabolite (**C**), the nitrones (**D** and **E**), the lactam metabolite (**F**) and the hydroxylated and *O*-dealkylated metabolite (**G**). Comparison of the product ion spectra of the metabolites **B–G** with that of the parent compound **A** indicates that the product ion spectra are compatible with the assigned structures.

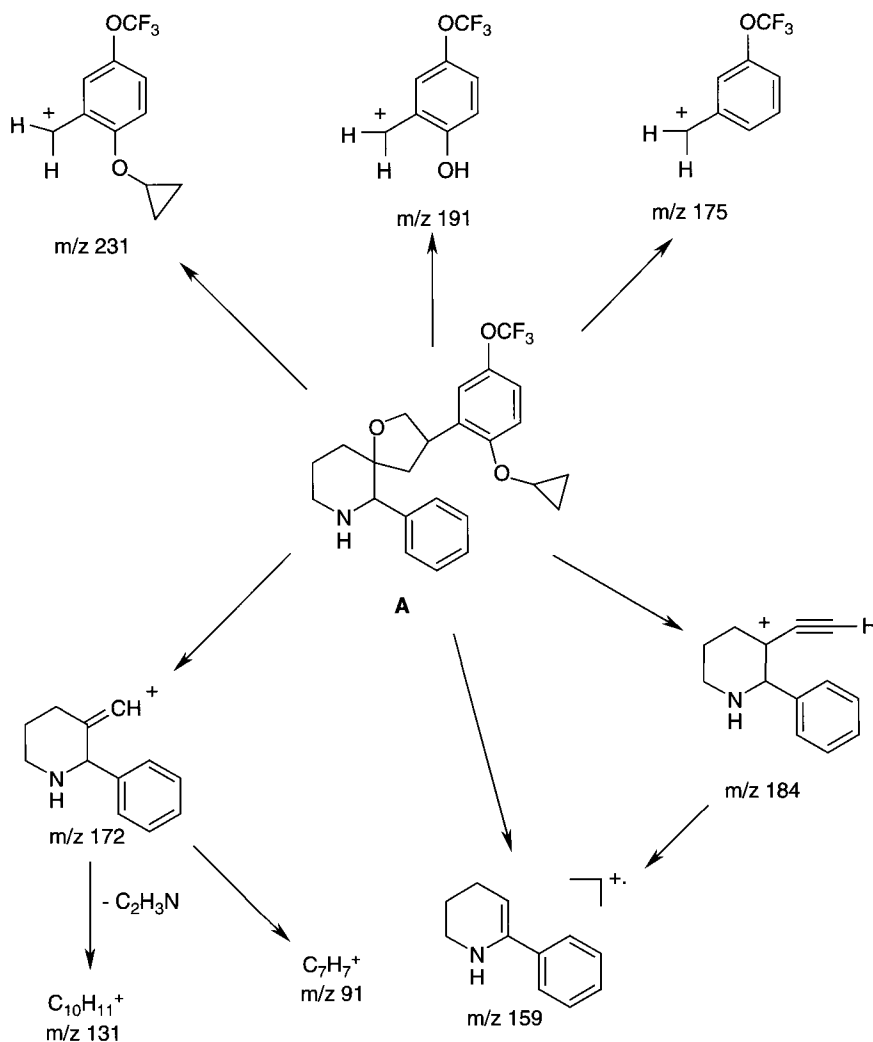
Table 4.

Assignment of the fragment ions observed in the product ion spectrum of protonated compound **A**, $\text{C}_{24}\text{H}_{26}\text{NO}_3\text{F}_3$, using the micromass Q-TOF II

Fragmentation (Da)	Observed mass (Da)	Formula assignment	Theoretical mass (Da)	Error (ppm)
416	416.1839	$\text{C}_{24}\text{H}_{25}\text{NO}_2\text{F}_3$	416.1837	0.5
231	231.0628	$\text{C}_{11}\text{H}_{10}\text{O}_2\text{F}_3$	231.0633	-2.2
215	215.0325	$\text{C}_{10}\text{H}_6\text{O}_2\text{F}_3$	215.0320	2.4
203 ^a	203.0677	$\text{C}_{10}\text{H}_{10}\text{OF}_3$	203.0684	-3.1
203 ^a	203.0304	$\text{C}_9\text{H}_6\text{O}_2\text{F}_3$	203.0320	-7.8
191	191.0325	$\text{C}_8\text{H}_6\text{O}_2\text{F}_3$	191.0320	2.4
184	184.1137	$\text{C}_{13}\text{H}_{14}\text{N}$	184.1126	5.8
175	175.0378	$\text{C}_8\text{H}_6\text{OF}_3$	175.0371	4.4
172	172.1136	$\text{C}_{12}\text{H}_{14}\text{N}$	172.1126	5.4
159	159.1053	$\text{C}_{11}\text{H}_{13}\text{N}$	159.1048	3.4
131	131.0873	$\text{C}_{10}\text{H}_{11}$	131.0861	9.1
91	91.0526	C_7H_7	91.0548	-23.9 ^b

^aThe signal at m/z 203 was composite.

^bThe signal at m/z 91 was outside the calibrated mass range resulting in a larger error.

**Figure 4.**

Tentative structural assignments for the most informative fragmentation pathways observed for protonated compound A upon collision-induced dissociation

The turnover of compound A in rat hepatocytes was only 30% and, therefore, the most abundant signal (at a retention time of 23.8 min) is the parent compound, A. The radiochromatogram is presented in Fig. 5 and the three metabolites eluting at retention times of 27.0, 29.8 and 32.8 min correspond to the two nitrones (D and E) and the lactam (F), respectively, based on comparison of the product ion spectra with those of the authentic standards. In addition, three minor metabolites were observed at retention times of 10.0, 15.2 and 32.8 min. The product ion spectrum

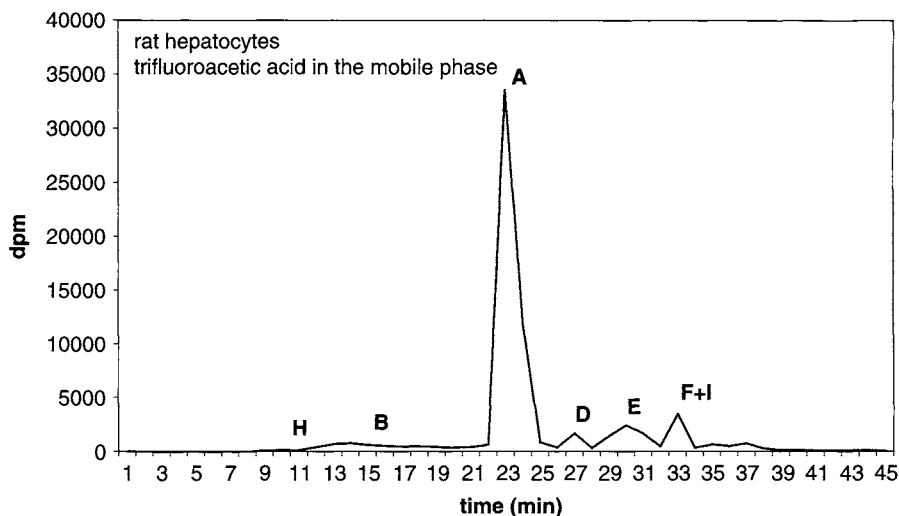


Figure 5.

HPLC-radiochromatogram of ^{14}C -labeled compound **A** and its metabolites generated in rat hepatocytes. The liquid chromatography mobile phase contained trifluoroacetic acid

of the metabolite at 15.2 min indicates that this was the *O*-dealkylated metabolite (**B**). The MS and MS/MS spectra of the metabolite eluting at 10.0 min indicate that the molecular weight of the metabolite is 585 Da and that loss of 176 Da occurs upon collision-induced dissociation. These data suggest that this metabolite (**H**) is a glucuronide of the hydroxylated and *O*-dealkylated metabolite (**G**, retention time = 13.0 min). Definitive structural assignment of the metabolite eluting at 32.8 min (tentatively assigned as metabolite **I**) was not possible. The mass spectrum indicates a molecular weight of 463 Da and signals at m/z 175, 191, 203 and 215 in the product ion spectrum imply that 30 Da has been added to the phenyl-piperidine moiety of the molecule (see below for more details).

The radiochromatogram obtained from rat plasma following oral or intravenous dosing with ^{14}C -labeled **A** diluted with unlabeled compound **A** differs significantly from that obtained with hepatocytes (compare Figs. 5 and 6). The signal corresponding with the parent compound was relatively weak and the major component in plasma was a new metabolite (**J**) eluting later (at 35.9 min) than all metabolites observed in rat hepatocytes. The mass spectrum of metabolite **J** contains signals at m/z 447, 465, 482 and 487, which correspond to $[\text{J} + \text{H} - \text{H}_2\text{O}]^+$, $[\text{J} + \text{H}]^+$, $[\text{J} + \text{NH}_4]^+$ and $[\text{J} + \text{Na}]^+$ ions. Thus, the molecular weight of metabolite **J** is 464 Da. Note that compounds with a low-proton affinity (due to the absence of a basic nitrogen atom) frequently give rise to $[\text{M} + \text{NH}_4]^+$ and $[\text{M} + \text{Na}]^+$ signals, which are more abundant than the $[\text{M} + \text{H}]^+$ signal. These data were obtained with an acidic mobile phase containing 0.1% trifluoroacetic acid. Without trifluoroacetic

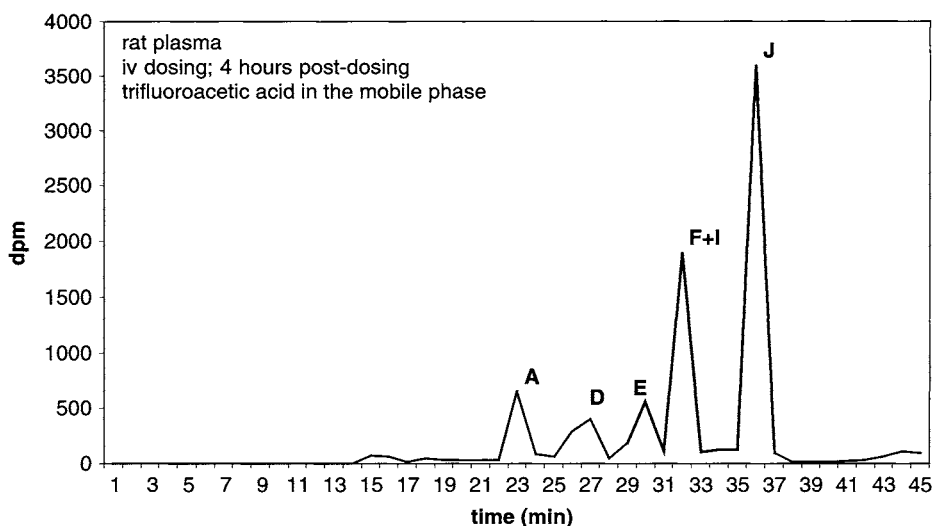


Figure 6.

HPLC-radiochromatogram of ^{14}C -labeled compound **A** and its metabolites present in rat plasma following intravenous administration at 10 mg/kg. The liquid chromatography mobile phase contained trifluoroacetic acid

acid in the mobile phase, the parent compound, **A**, eluted slightly later (at 29.6 min) and metabolite **J** eluted much earlier (at 23.1 min). The major change in the retention time of metabolite **J** suggests that this metabolite contains a carboxylic acid moiety. At low pH, the latter metabolite will be neutral, which results in more interaction with the C18 stationary phase and a longer retention time. Without trifluoroacetic acid in the mobile phase, it was also possible to obtain mass spectrometric data in the negative ion mode; an intense signal at m/z 463 was obtained for metabolite **J**, which confirms the molecular weight derived from the positive ion mode data.

The positive ion mode product ion spectrum of metabolite **J** contains signals at m/z 175, 191, 203 and 215, which were also observed in the product ion spectrum of the parent compound. Thus, the metabolic biotransformation must have occurred at the phenyl piperidine moiety of the molecule. The most intense signal, m/z 105, corresponds to $[\text{C}_6\text{H}_5-\text{C}=\text{O}]^+$ ions, which suggests oxidative ring opening of the piperidine ring. The negative ion product spectrum provides little additional information; the spectrum was dominated by a signal at m/z 85, which corresponds with $[\text{F}_3\text{C}-\text{O}]^-$ anions. Combination of these data with knowledge of biotransformations feasible for piperidine-containing compounds led to the keto acid structure presented in Fig. 7. This was confirmed by the ^1H NMR spectrum of the isolated metabolite **J**. The signals due to the aliphatic protons at the 2 and 6 positions of the piperidine ring in the parent compound disappeared and the splitting patterns of the protons (due to proton-proton interaction) at the 5 position of the piperidine ring and the ortho positions on the phenyl ring changed significantly. The latter aromatic protons

were also displaced downfield, which suggests the presence of an adjacent carbonyl moiety and, consequently, opening of the piperidine ring. Thus, the MS and NMR data combined suggest that metabolite **J** has the keto acid structure. The oxidative deamination mechanism presented in Fig. 8 is proposed for formation of metabolite **J** and a similar mechanism has been presented for the metabolism of *N*-deacetyl ketoconazole by Rodriguez *et al.* (1999). Many of the metabolic intermediates presented in Figure 8, such as the secondary hydroxylamine (**C**, minor component) and the nitrones (**D** and **E**), were observed in rat plasma after dosing with compound **A**. A metabolite with a molecular weight of 463 Da (**I**; retention time = 32.8 min) was observed in rat plasma as well as in rat hepatocyte incubations (see above). The product ion spectrum contains signals at *m/z* 175, 191, 203 and 215, which implies that the trifluoromethoxy phenyl moiety is intact and that 30 Da has been added to the phenyl piperidine moiety. The most intense signal in the product ion spectrum is

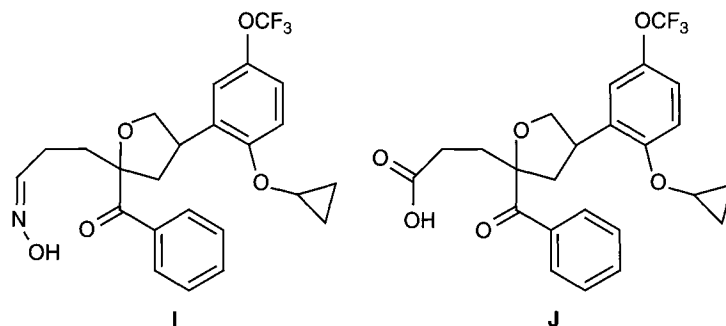


Figure 7.
The structures of metabolites **I** and **J**

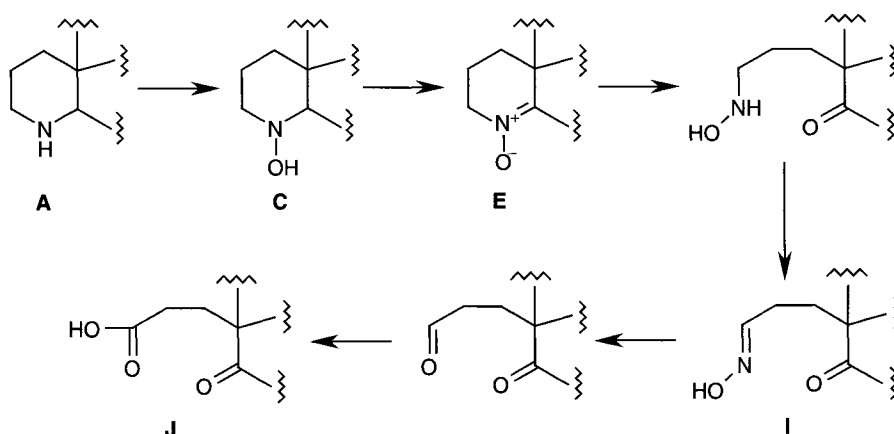


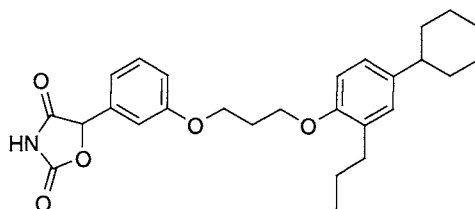
Figure 8.
The proposed mechanism for oxidative deamination of compound **A**

at m/z 105, which was also observed for metabolite **J**. Thus, metabolite **I** could be the oxime presented in Fig. 7, which is the analog of the oxime intermediate proposed for the metabolism of *N*-deacetyl ketoconazole (Rodriguez *et al.*, 1999).

Thus, mass spectrometric data were employed to elucidate the metabolism of [3R,5R,6S]-3-(2-cyclopropyloxy-5-trifluoromethoxyphenyl)-6-phenyl-1-oxa-7-azaspiro [4.5]decane and significantly different metabolic profiles were observed for rat hepatocytes and rat plasma with the major circulating metabolite, **J**, being generated by oxidative deamination of the piperidine ring. However, it is not clear whether the high-plasma levels of metabolite **J** are due to rapid formation of metabolite **J** or slow elimination of metabolite **J** from systemic circulation.

6.5.2. Metabolism of a Potent PPAR γ Agonist

Diabetes mellitus is a major threat to human health and the number of diabetics continues to increase (Zimmet *et al.*, 2001). The most common form of diabetes is type 2 diabetes, which is characterized by insulin resistance and/or abnormal insulin secretion. Hyperglycemia may lead to nephropathy, neuropathy, retinopathy and atherosclerosis. Control of blood glucose levels can be achieved with oral hypoglycemic agents, such as sulphonylureas, metformin, peroxisome proliferator-activated receptor- γ (PPAR γ) agonists, α -glucosidase inhibitors and insulin (Moller, 2001). Upon ligand binding, the nuclear hormone receptor PPARs regulate specific gene expression by binding to peroxisome proliferator responsive elements after heterodimerization with another nuclear receptor, retinoid X receptor (Berger and Moller, 2002). The nuclear hormone receptor PPAR γ governs expression of genes involved in the regulation of glucose and lipid metabolism. The ultimate outcome of administration of a PPAR γ agonist is an increase in the sensitivity of certain tissues toward insulin, which enhances glucose metabolism and inhibits hepatic gluconeogenesis. Troglitazone, pioglitazone and rosiglitazone, all thiazolidinediones (TZDs), are PPAR γ agonists and have shown clinical efficacy, but troglitazone was withdrawn because of idiosyncratic, but severe, hepatotoxicity. As an alternative to TZDs, oxazolidinediones (OZDs) have been identified as PPAR γ agonists by Desai *et al.* (2003). Here, the *in vitro* metabolism of a new PPAR γ agonist, compound **K**, is described.



K, 451 Da

Compound **K** ionizes better in the negative than the positive ion mode due to the acidic nature of the OZD moiety. This facilitated metabolite identification because signals

due to endogenous material are usually less abundant in the negative ion mode. The product ion spectrum of the $[\mathbf{K} - \text{H}]^-$ ions at m/z 450 was dominated by an intense signal at m/z 42, which can be ascribed to $[\text{N}\equiv\text{C}-\text{O}]^-$ from the OZD ring; the abundance of all other fragment ions (m/z 191, 203 and 217) was less than 5% of the intensity of the m/z 42 signal. Thus, negative ion mode data provided little structural information.

In the positive ion mode, the $[\mathbf{K} + \text{H}]^+$ signal at m/z 452 was very small, but the $[\mathbf{K} + \text{NH}_4]^+$ signal at m/z 469 was more abundant. Fragmentation of the $[\mathbf{K} + \text{NH}_4]^+$ ions gave rise to several structure characteristic signals, including m/z 234, 190, 177 and 83, and the nature of these ions is described in Fig. 9. The intensity of m/z 83 ($[\text{C}_6\text{H}_{11}]^+$), albeit small, defined the cyclohexane ring.

Thus, metabolites of compound **K** were identified in a three-step process:

1. Identification of metabolites via LC-MS in the negative ion mode.
2. Confirmation of metabolites via LC-MS/MS in the negative ion mode using m/z 42 precursor ion detection.
3. Characterization of metabolites via LC-MS/MS in the positive ion mode using $[\mathbf{K} + \text{NH}_4]^+$ and/or $[\mathbf{K} + \text{H}]^+$ ions as precursor.

Incubation of compound **K** with rat, dog, monkey and human liver microsomes resulted in a large extent of metabolism with the major pathways being associated with oxidation of the cyclohexyl ring. (Other, mostly minor, metabolic processes include oxidation of the propyl side chain and opening of the OZD ring.) Figure 10 shows the extracted ion chromatograms from rat, dog, monkey and human liver microsomal samples for the m/z 466 $[\mathbf{K} + \text{O} - \text{H}]^-$ ions. Generally, microsomes from all four species form the same hydroxylated metabolite, but there are striking quantitative differences. In the positive ion mode, the corresponding m/z 468 ($[\mathbf{K} + \text{O} + \text{H}]^+$) signals were small, but signals at m/z 485 ($[\mathbf{K} + \text{O} + \text{NH}_4]^+$) and 450 ($[\mathbf{K} + \text{O} - \text{H}_2\text{O} + \text{H}]^+$) were present. The abundance of the m/z 450 signal indicates that the protonated hydroxy metabolites are relatively unstable and loss of H_2O prevails, which suggests that hydroxylation of aliphatic carbon atoms, but not aromatic

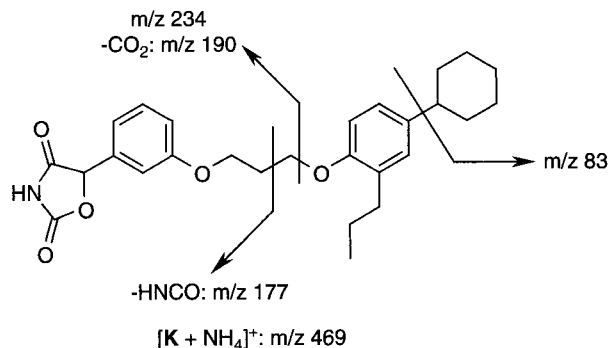


Figure 9.

Tentative structural assignments for the most informative fragmentation pathways observed for $[\mathbf{K} + \text{NH}_4]^+$ upon collision-induced dissociation

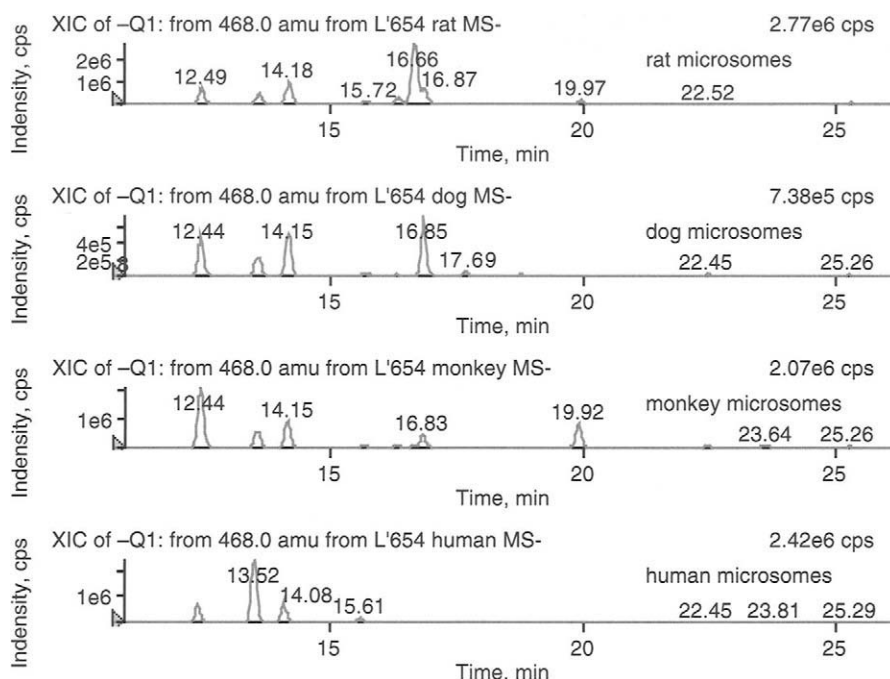


Figure 10.

Extracted ion chromatograms for the m/z 466 $[K + O - H]^-$ ions from compound **K** incubated with rat, dog, monkey and human liver microsomes

carbon atoms, has taken place. The positive ion mode product ion spectra of the $[K + O + NH_4]^+$ ions from the four hydroxylated metabolites eluting at 12.4, 13.5, 14.2 and 16.8 min had characteristic signals at m/z 234, 190, 177 and 81. The signal at m/z 81 corresponds with $[C_6H_{11} + O - H_2O]^+$, which is indicative of hydroxylation of the cyclohexane ring in multiple positions. However, LC-MS/MS does not provide regiochemical information regarding hydroxylation of the cyclohexane ring. Relatively, small quantities of several $[K + 14 Da]$ metabolites were detected as well and all product ion spectra had a signal at m/z 97. The signal at m/z 97 corresponds with $[C_6H_9O]^+$, which is indicative of ketone formation in multiple positions on the cyclohexane ring.

Compound **K** was also incubated with recombinant cytochrome P450 2C8, 2C19 and 3A4 enzymes. The turnover was greatest with 2C8 followed by 2C9 and the turnover with 3A4 was small. The respective extracted ion chromatograms for the m/z 466 $[K + O - H]^-$ ions are presented in Fig. 11 and, again, the profiles, in particular the regions between 10 and 20 min, are quantitatively quite distinct. The hydroxylated metabolites generated by CYP2C8 and CYP2C19 feature prominently in the extracted ion chromatogram generated for human liver microsomes (Figs. 10 and 11). The product ion spectra obtained in the positive ion mode indicate that the major hydroxylated metabolites involve hydroxylation of the cyclohexane ring.

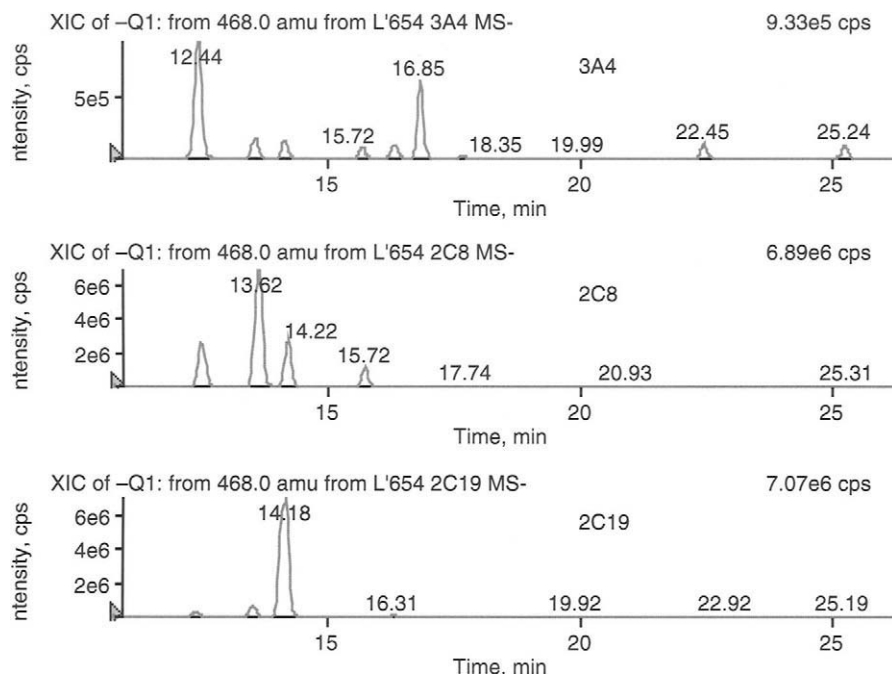


Figure 11.

Extracted ion chromatograms for the m/z 466 $[\mathbf{K} + \text{O} - \text{H}]^-$ ions from compound **K** incubated with recombinant cytochrome P450 3A4, 2C8 and 2C19 enzymes

To obtain more information about the regiochemistry and stereochemistry of the hydroxylated metabolites, compound **K** was incubated in a bioreactor (Rushmore *et al.*, 2000) with the two cytochrome P450 enzymes which had the most turnover, i.e. CYP2C8 and CYP2C19, followed by isolation of the most abundant metabolites and analysis by ^1H NMR. Two chromatographic fractions each were isolated for CYP2C8 (13.6 and 14.2 min) and CYP2C19 (13.6 and 14.2 min). Chemical shifts and coupling constants in the ^1H NMR spectrum indicated that CYP2C8 forms two equatorial hydroxy metabolites and CYP2C19 forms two axial hydroxy metabolites (Fig. 12).

These data indicate that CYP enzymes from different species display subtle quantitative differences in the regioselectivity for hydroxylation of the cyclohexane ring. In addition, the human CYP enzymes 2C8 and 2C19 possess stereoselectivity for hydroxylation of the cyclohexane ring.

6.5.3. Metabolism of an Antipsychotic Drug Ziprasidone

Schizophrenia is a complex disorder characterized by thought disturbances, auditory hallucinations and inappropriate effects (Howard and Seeger, 1993). While the classical antipsychotic drugs of the phenothiazine and butyrophenone classes are

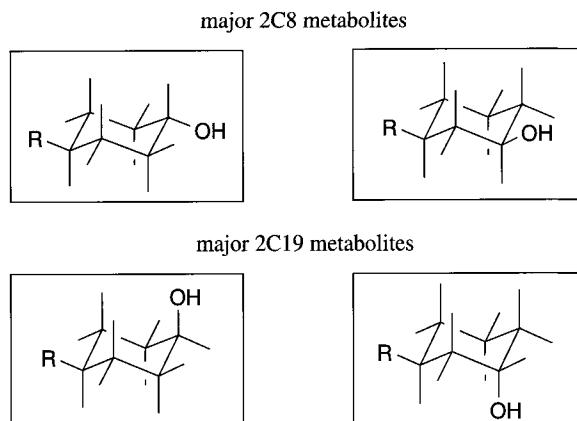


Figure 12.

The structures of major hydroxylated metabolites of compound **K** in recombinant CYP2C8 and CYP2C19

effective in the treatment of schizophrenia, their usage is commonly associated with extrapyramidal side effects (Tarsey, 1983). In addition, these drugs are not effective in all patients or against both positive and negative symptoms of schizophrenia (Ortiz and Gershon, 1986). Laboratory and clinical findings have suggested that antagonism of serotonin 5-HT_{2C} receptors in the brain limits the undesirable motor side effects associated with dopamine receptor blockade and improves efficacy against the negative symptoms of schizophrenia (Meltzer, 1995). Ziprasidone, a substituted benzisothiazolyl-piperazine analog, was recently approved for the treatment of schizophrenia (Fig. 13). It exhibits potent and highly selective antagonistic activity on the dopamine D₂ and serotonin 5-HT_{2A} receptors. It also has high affinity for the 5-HT_{1A}, 5-HT_{1D} and 5-HT_{2C} receptor subtypes that could contribute to the overall therapeutic effect (Howard *et al.*, 1994). Preclinical ADME studies were needed to support the safety assessment package for registration of this new drug. Here, the strategies for the identification of metabolites of ziprasidone in rats are described.

6.5.3.1. Use of Two Different Radiolabels

The metabolism of tiospirone, a structurally related analog of ziprasidone (Fig. 13), has been described earlier (Mayol *et al.*, 1991). One of its main metabolic pathways, *N*-dealkylation of the butyl group attached to the piperazinyl nitrogen, resulted in the cleavage of the molecule into two major portions. However, these studies were conducted using tiospirone labeled with ¹⁴C at the piperazine ring and hence only the metabolites containing the benzisothiazole piperazine (BITP) moiety were monitored. It is desirable to trace both fragments by providing each with a different label. Thus, we studied the metabolism of ziprasidone in preclinical species and humans after administration of a mixture of ziprasidone labeled with ¹⁴C at the C-2 of the ethyl group attached to the

piperazinyl nitrogen and ziprasidone labeled with ^3H at the C-7 position of the benzisothiazole (Prakash *et al.*, 1997). The use of two labels not only facilitated the tracing of metabolites formed through *N*-dealkylative cleavage of ziprasidone, but also aided their identification. A total of 11 peaks were detected in the radiochromatograms in the rat urine (Fig. 14). Metabolites **M1**, **M2** and **M3** were detected only in the ^3H radiochromatogram indicating that they were cleavage products associated with the benzisothiazole moiety. On the other hand, metabolite **M4** was detected mainly in the ^{14}C radiochromatogram with a smaller peak in ^3H radiochromatogram representing spillover, indicating that it was also a cleaved metabolite but containing the oxindole moiety. The remaining metabolites, **M6**, **M7**, **M8**, **M9** and **M10**, were detected by peaks of similar

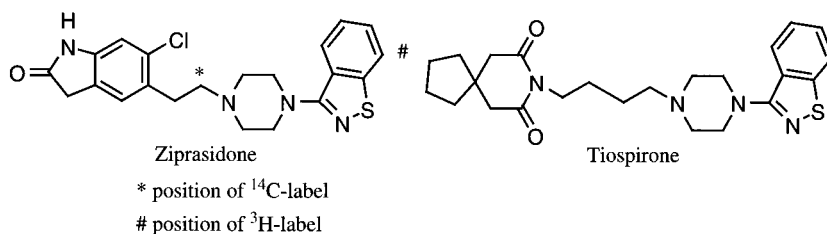


Figure 13.
Structures of ziprasidone and a structurally related analog tiospirone

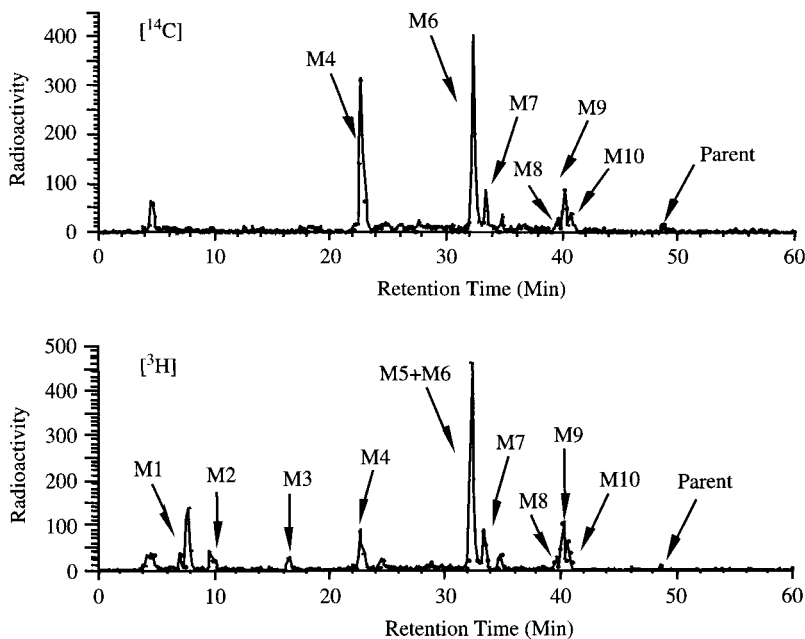


Figure 14.
HPLC-radiochromatograms of ziprasidone metabolites in rat urine

heights in both radiochromatograms, suggesting that they did not undergo cleavage at the piperazinyll nitrogen and, therefore, are expected to be dual labeled.

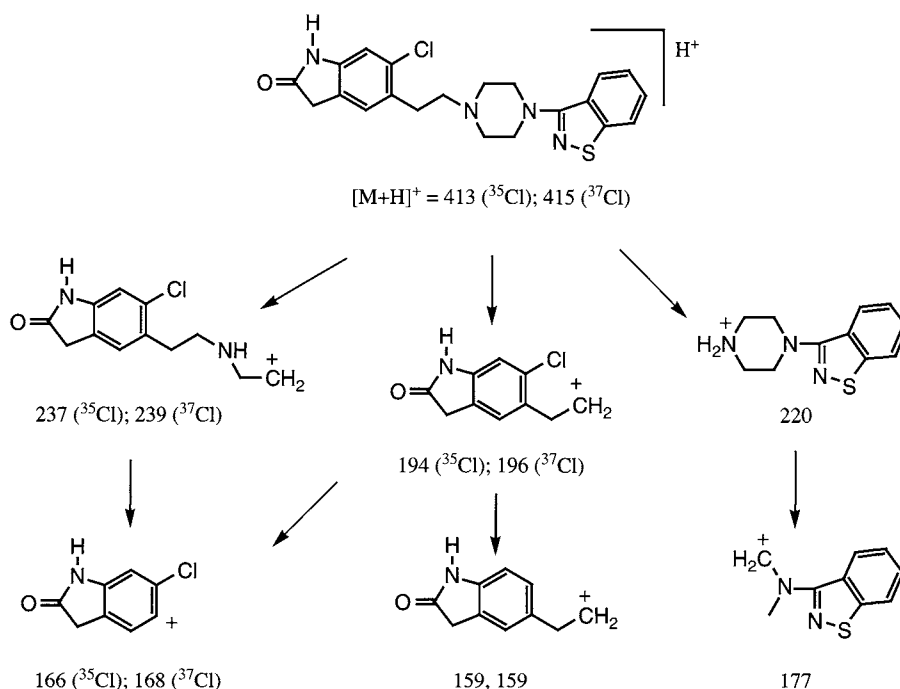
6.5.3.2. Precursor Ion Spectrum

Ziprasidone generated a strong pseudomolecular ion $[M + H]^+$ at m/z 413. The product ion mass spectrum of m/z 413 showed signals at m/z 220, 194, 177, 166 and 159. The two diagnostic fragment ions at m/z 220 and 194 resulted from the cleavage of the C-N (piperazine) bond and corresponded to $[BITP + H]^+$ and $[\text{oxindole-CH}_2\text{CH}_2]^+$, respectively. The other fragment ions at m/z 177 and 159 were due to losses of 43 ($\text{CH}_3\text{N}=\text{CH}_2$) and 35 Da (Cl) from the ions at m/z 220 and 194, respectively (Fig. 15). The assignment of these ions was confirmed by the parallel product ion spectrum of m/z 415 ($[M + H]^+$, ^{37}Cl), which gave fragment ions at m/z 220, 196, 177, 166 and 159. Precursor ion scanning (see Fig. 2) of m/z 194 provided molecular ion information for seven metabolites from rat urine (Fig. 16). Product ion spectra of the protonated molecules provided structurally significant fragment ions. Metabolites **M1**, **M2**, **M3**, **M4** and **M5** were identified as BITP-sulfone, BITP-sulfoxide, BITP-sulfone-lactam, chlorooxindole acetic acid and BITP, respectively. Metabolites **M6**, **M8**, **M9** and **M10** were characterized as *S*-methyl-dihydro-ziprasidone-sulfoxide, ziprasidone sulfone, *S*-methyl-dihydro-ziprasidone and ziprasidone sulfoxide, respectively (Fig. 17).

6.5.3.3. Differentiation of Isobaric Metabolites

Metabolite **M9** showed a protonated molecule at m/z 429, the same as of **M10**, suggesting that **M9** and **M10** were isobars. The product ion spectrum of **M9** (m/z 429) showed fragment ions at m/z 280, 263, 219, 194, 150 and 123. The ion at m/z 280 corresponds to a charge-initiated fragmentation of the piperazinyll nitrogen benzisothiazole carbon bond with the expulsion of the benzisothiazole +16 Da moiety as a neutral molecule. The ion at m/z 150 resulted from the cleavage of the same nitrogen-carbon bond with charge retention on the benzisothiazole +16 Da moiety and suggested modification of the benzisothiazole ring. The assignment of these ions was confirmed by a parallel product ion spectrum of m/z 431 ($[M + H]^+$, ^{37}Cl), which gave fragment ions at m/z 282, 265, 196, 150 and 123. These results strongly suggest that the oxidation had occurred at the benzisothiazole moiety. Based on addition of 16 Da to the benzisothiazole moiety, three structures were originally considered for **M9**: oxidation at the nitrogen of the benzisothiazole ring to form an *N*-oxide, **1**; aromatic hydroxylation of the benzisothiazole moiety, **2** and reductive cleavage of the benzisothiazole followed by methylation of the resulting thiophenol to form **3** (Fig. 18).

Treatment of **M9** with aqueous TiCl_3 , *tert*-butyldimethylsilyl-*N*-trifluoroacetamide or diazomethane did not change the HPLC retention time or the molecular ion of metabolite **M9**. These results indicate that **M9** was neither an *N*-oxide (**1**) nor

**Figure 15.**

Tentative structural assignments for the most informative fragment ions of protonated ziprasidone

a hydroxy metabolite (**2**). Based on these data, **M9** was identified as *S*-methyl-dihydro-ziprasidone, **3**, formed by the reductive cleavage of the benzisothiazole moiety. Accurate mass measurements obtained with a Q-TOF mass spectrometer provided additional information. Table 5 summarizes the molecular formula assignments for the protonated molecule of ziprasidone and its two isobaric metabolite **M9** and **M10**. The significant difference between the observed m/z value for protonated **M9** and **M10** indicates that **M9** and **M10** have different molecular formulas, which is in keeping with their structural assignments (see Fig. 17).

6.5.4. Biotransformation of an Anxiolytic Drug Candidate, CP-93,393

CP-93,393, a pyrimidinylpiperazine analog (Fig. 19), exhibits highly selective 5-hydroxytryptamine (5-HT) serotonin autoreceptor agonist activity (Schmidt *et al.*, 1995). It differs in mechanism from the benzodiazepines, which are generally believed to act by potentiating the neural inhibition mediated by GABA, but bears a mechanistic relationship to a new class of nonbenzodiazepines anxiolytics, azapirones (Rollema *et al.*, 1996). But unlike these agents, CP-93,393 itself exhibits

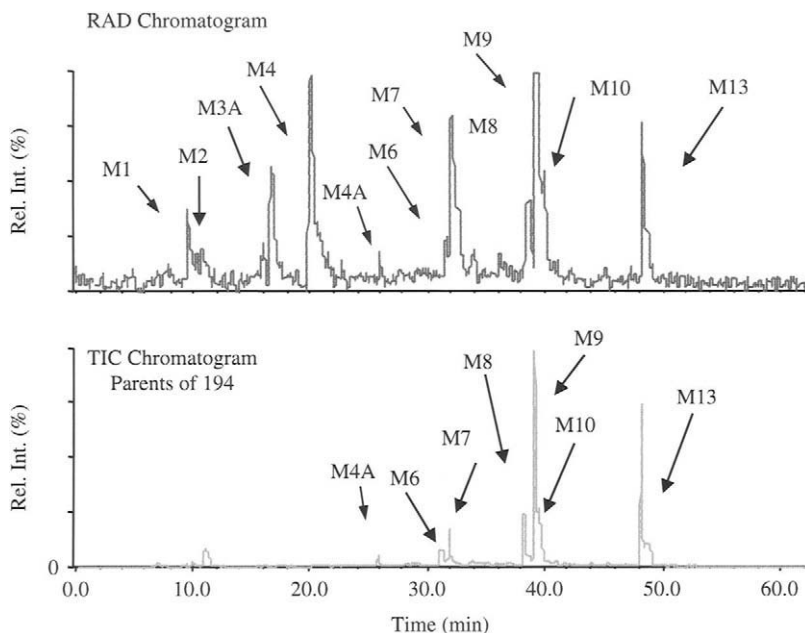


Figure 16.

HPLC-radiochromatogram and TIC chromatogram (precursor ion spectrum of m/z 194) of ziprasidone metabolites in rat urine

α 2-adrenoceptor antagonist activity that may have therapeutic relevance for antidepressant activity. It is being evaluated for its effectiveness in the treatment of generalized anxiety disorder and major depressive disorder. Here, we describe the metabolism of CP-93,393, {1-(2-pyrimidin-2-yl)-octahydro-pyrido[1,2-a]pyrazin-7-ylmethyl)-pyrrolidine-2,5-dione, in rat urine as well as in monkey liver microsomes.

CP-93,393 and 15 metabolites were detected in the radiochromatogram from a urine sample of rats following oral administration of ^{14}C -labeled CP-93,393 (Fig. 20). The identification of metabolites was achieved by chemical derivatization, β -glucuronidase/sulfatase treatment and LC-MS/MS (Prakash and Soliman, 1997). Based on the structures of hydroxylated metabolites, four primary metabolic pathways of CP-93,393 were identified: hydroxylation at the pyrimidine ring (**M15**), hydroxylation at the succinimide ring (**M16**), hydroxylation α to the nitrogen of the piperazine ring (**M10**) and hydrolysis of imide bond of the succinimide ring (**M9**). The major oxidative metabolites were excreted as sulfate and/or glucuronide conjugates (**M7**, **M12** and **M13**) (Fig. 21).

CP-93,393 and metabolites displayed very intense protonated molecules, $[\text{M} + \text{H}]^+$. The product ion mass spectra of the $[\text{M} + \text{H}]^+$ provided very characteristic fragment ions; at least six structurally informative fragment ions were observed for CP-93,393 and its hydroxylated analogs (fragments a–f, Fig. 22A). For CP-93,393,

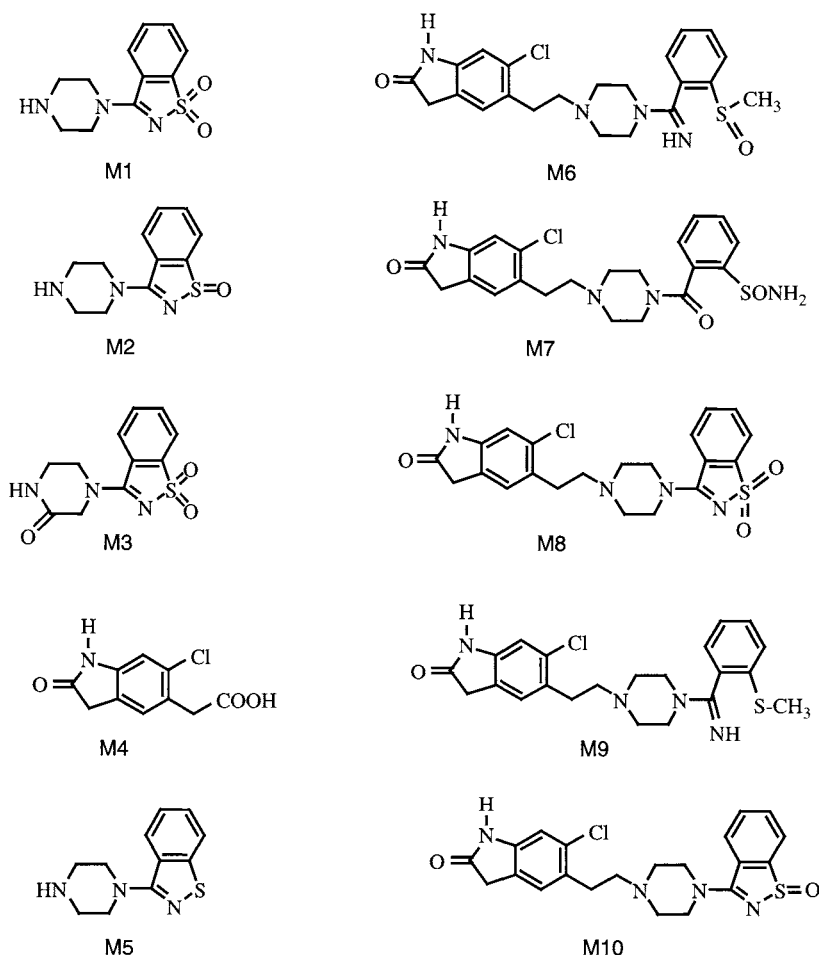


Figure 17.
Proposed structures of metabolites of ziprasidone in rats

fragmentation occurred across the piperazine ring to give ions at m/z 235 (fragment a), 209 (fragment b) and 195 (fragment c) with charge retention at the succinimidyl part of the molecule. Hydroxylation at the succinimide ring, such as **M16**, resulted in these ions appearing 16 Da higher, at m/z 251 (fragment a), 225 (fragment b) and 211 (fragment c). Absence of substitution at the succinimide moiety, such as **M10**, resulted in these ions being observed at the same m/z values as CP-93,393: m/z 235, 209 and 195 (fragments a, b and c, respectively). Two fragmentation reactions across the piperazine ring with charge retention at the pyrimidine portion of the CP-93,393 gave ions at m/z 136 (fragment d) and 122 (fragment e). Therefore, hydroxylation at the pyrimidine ring, such as **M15**, resulted in ions at m/z 152 and 138, 16 Da higher than CP-93,393. In addition, a very characteristic fragment ion due

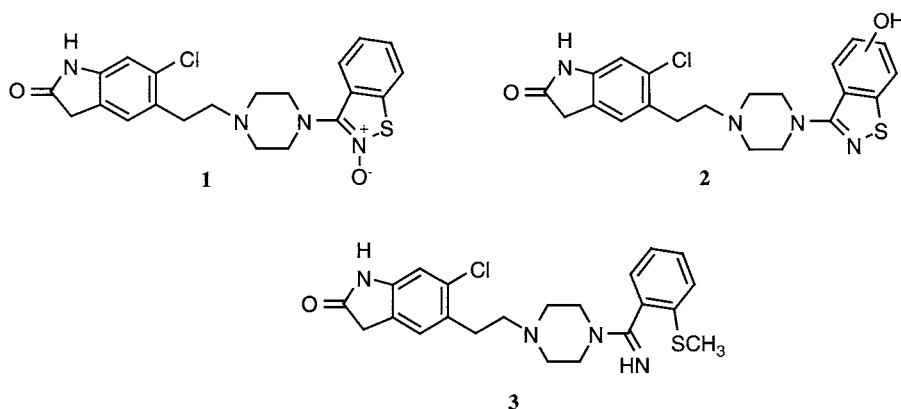


Figure 18
Possible structures of metabolite **M9**

Table 5.

Accurate mass measurements and molecular formula assignments of ziprasidone and its two isobaric metabolites **M9** and **M10** obtained with a micromass Q-TOF II

Compound	Observed mass (Da)	Formula assignment	Theoretical mass (Da)	Error (ppm)
Ziprasidone	413.1205	C ₂₁ H ₂₂ N ₄ O ₂ SCl	413.1203	0.4
M9	429.1520	C ₂₂ H ₂₆ N ₄ O ₂ SCl	429.1516	0.9
M10	429.1151	C ₂₁ H ₂₂ N ₄ O ₂ SCl	429.1152	-0.3

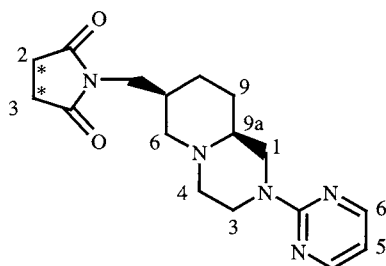


Figure 19.
Structure of CP-93,393 (* indicates the positions of the ¹⁴C-labels)

to the loss of succinimide ring was observed for most of the compounds (fragment f, Fig. 22A).

For hydrolysis products, such as 1-(2-pyrimidin-2-yl-octahydro-pyrido[1,2-a]pyrazin-7-ylmethyl)-succinamic acid (NPMSA), fragmentation also occurred across

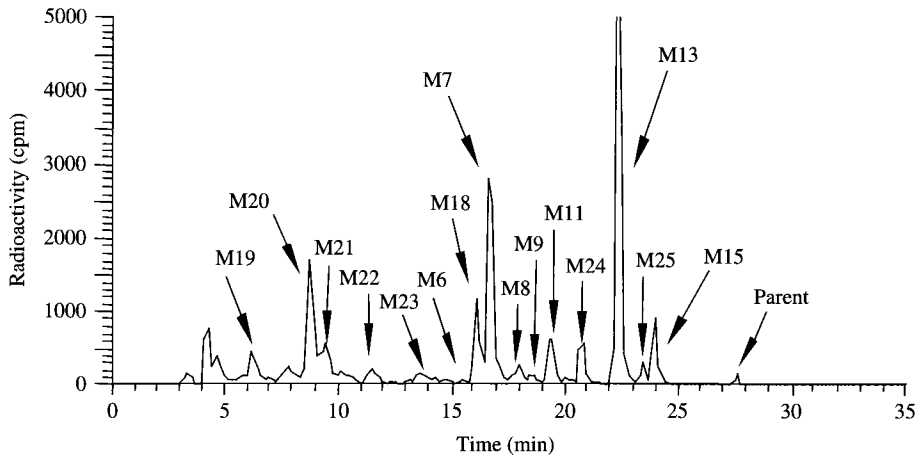


Figure 20.

HPLC-radiochromatogram of urinary metabolites of ^{14}C -labeled CP-93,393 following oral administration to rats

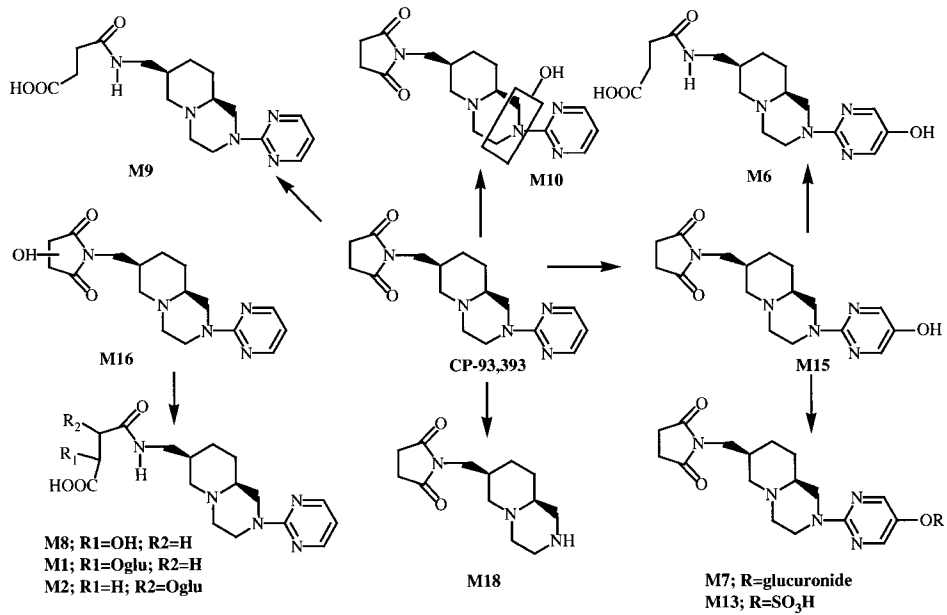
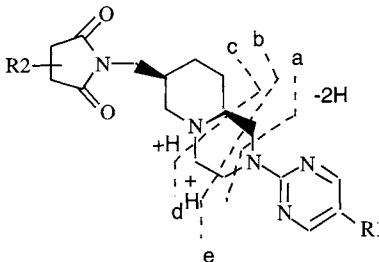


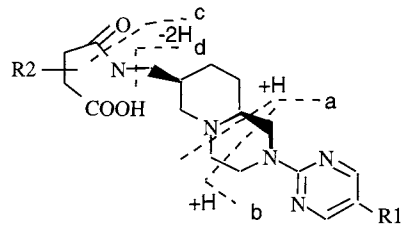
Figure 21.

Proposed biotransformation pathways of CP-93,393 in rats



Compound	R1	R2	MH ⁺	a	b	c	d	e	f
CP-93,393	H	H	330	235	209	195	136	122	231
5-OH-CP-93,393	OH	H	346	235	209	195	152	138	247
2 or 3-OH-CP-93,393	H	OH	346	251	225	211	136	122	231

(A)



Compound	R1	R2	MH ⁺	a	b	c	d
NPMISA	H	H	348	136	122	248	231
NHPMISA	OH	H	364	152	136	264	247
2 or 3-NPMHSA	H	OH	364	136	122	248	231

(B)

Figure 22.

Fragmentation pattern of protonated CP-93,393 and its putative metabolites

the piperazine ring with charge retention only at the pyrimidine portion of the molecule, generating characteristic ions at m/z 136 (fragment a) and at m/z 122 (fragment b). An additional fragment ion at m/z 248 resulted from the cleavage of the amide bond (fragment c). Hydroxylation at the pyrimidine ring, such as 1-[2-(5-hydroxy-pyrimidin-2-yl)-octahydro-pyrido[1,2-a]pyrazin-7-ylmethyl]-succinamic acid (5-NHPMISA), resulted in ions at m/z 152 (fragment a), 138 (fragment b) and 264 (fragment c), all 16 Da higher than NPMISA. For 1-(2-pyrimidin-2-yl-octahydro-pyrido[1,2-a]pyrazin-7-ylmethyl)-2-hydroxy-succinamic acid (2-NPMHSA) and-(2-pyrimidin-2-yl-octahydro-pyrido[1,2-a]pyrazin-7-ylmethyl)-3-hydroxy-succinamic acid (3-NPMHSA), these fragment ions were observed at the same m/z values as observed for NPMISA (Fig. 22B).

Two metabolites **M1** and **M2** eluting at retention times of ~10.8 and 12.9 min correspond to isomeric glucuronides of 2-NPMHSA and 3-NPMHSA, respectively. The structures of these isomeric glucuronides were elucidated by constant neutral loss scanning and LC-MS/MS/MS (MS^3) techniques. The glucuronide conjugates were dissociated at the orifice and the resulting aglycones were subjected to collision-induced dissociation. The product ion spectrum of **M1** (m/z 364; generated at the orifice) gave fragment ions at m/z 318, 290, 248, 231, 136 and 122. The characteristic fragment ion at m/z 290 (loss of $-CH(OH)COOH$) indicates the presence of a hydroxy group α to the carboxyl moiety. On the other hand, the MS/MS/MS spectrum of **M2** showed fragment ions at m/z 304, 248, 136 and 122. The characteristic fragment ion at m/z 304 (loss of CH_3COOH from the ion at m/z 364; generated at the orifice) suggests the presence of a hydroxy group β to the carboxyl moiety.

The radiochromatogram obtained from monkey liver microsomes showed the presence of a metabolite, **M18**, which was not identified in rat urine. **M18** displayed a protonated molecule at m/z 294, 36 Da lower than that of the parent molecule. The fragment ions at m/z 252, 235, 209 and 195 in the product ion spectrum of **M18** indicate the modification of the pyrimidine ring. Furthermore, the fragment ion at m/z 252, generated via loss of 42 Da from the molecular ion, suggest the presence of an acetyl or a carboxamidino group (Fig. 23). H/D exchange and derivatization techniques were very useful for differentiating these structures. When H_2O was replaced with D_2O in the mobile phase, the full-scan mass spectrum of **M18** revealed

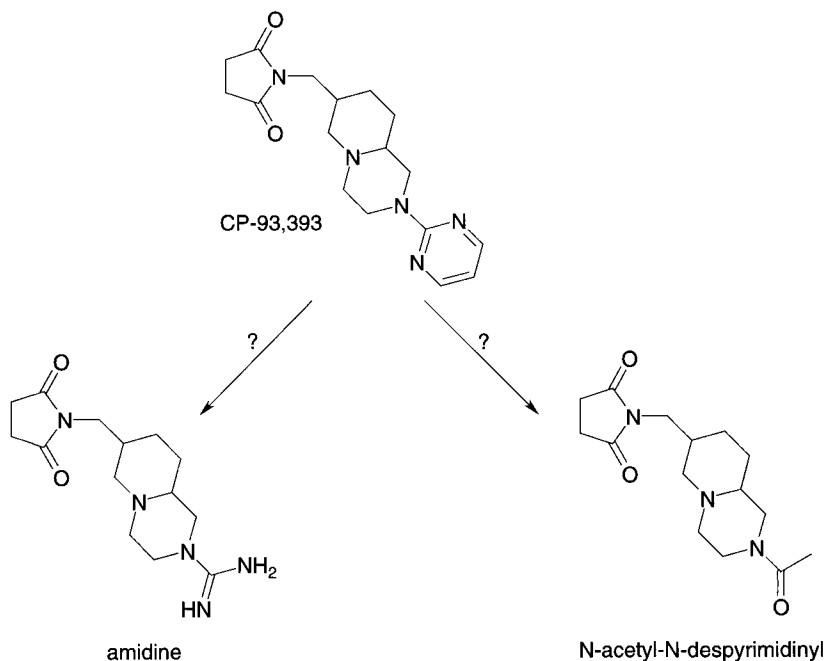


Figure 23.
Possible structures of metabolite **M18**

a molecular ion $[M_D + D]^+$ at m/z 294 (M_D represents the molecular weight following H/D exchange in D_2O), 4 Da higher than $[M_H + H]^+$. The increase of 4 Da is in agreement with the presence of three exchangeable hydrogen atoms, which is consistent with the carboxamidino analog structure for **M18**. The carboxamidine structure of **M18** was further confirmed by treatment with hexafluoroacetylacetone, which resulted in the formation of *bis*-trifluoromethyl-CP-93,393 (Fig. 24), a reaction characteristic for the detection of carboxamidines (Prakash and Cui, 1997). Comparison of the product ion spectrum of the derivatized metabolite with that of **M18** indicates that the product ion was compatible with the assigned structure.

6.6. Future Trends

Metabolite identification has proven to be of great value in drug discovery and development and LC-MS is the preferred analytical tool. However, metabolite identification is a labor-intensive activity and depends on the availability of highly skilled scientists. Software has recently become available to automate certain steps in the metabolite identification process (Lim *et al.*, 1999; Yu *et al.*, 1999). For example, after acquiring full scan MS data, the software will interrogate the MS data for anticipated metabolites considering the mass changes associated with the biotransformations listed in Tables 1 and 2. Subsequently, product ion spectra will automatically be acquired for tentatively identified biotransformations. Although this approach can be successful for *in vitro* samples (liver microsomes, hepatocytes, etc.), it is of limited use for *in vivo* samples because of the large amount of endogenous material present, which can have the same molecular weight as the anticipated metabolites. Correlating the full scan MS data of the sample of interest with those of an appropriate control sample ($t = 0$ min, minus NADPH, inactivated enzymes, etc.) will prevent acquisition of product ion spectra of endogenous components with the same molecular weight as anticipated metabolites. However, proper controls may not always be available and, sometimes, the drug affects the abundance of certain endogenous components. Although the software

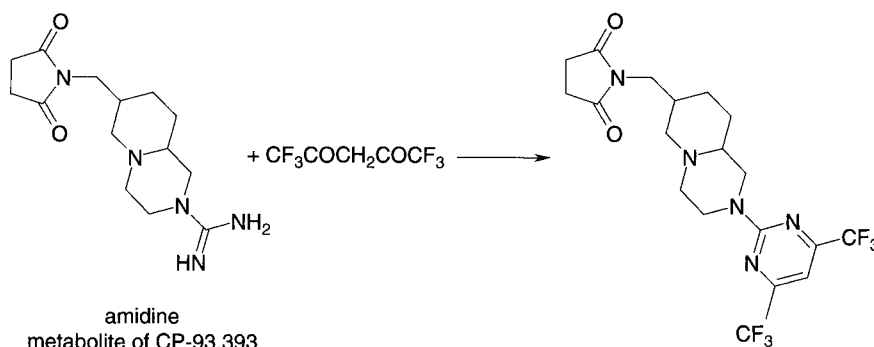


Figure 24.
Derivatization of **M18** with hexafluoroacetylacetone

can facilitate the experimental component of the metabolite identification process, ultimately interpretation of the spectra will still be the rate limiting. Thus, tools to automate data interpretation are urgently needed. Reliable *in silico* tools, which predict metabolite formation, are valuable as well and combining these with the LC–MS data acquisition software should provide a powerful combination.

Acknowledgments

The authors thank numerous former colleagues at Merck Research Laboratories, in particular Drs. Yanfeng Wang, Arun Agrawal and Maria Silva Elipe, and Drs. Amin Kamel, Dan Cui, Wayne Anderson, Keith McCarthy, Kathleen Zandi and Ms. Kim Johnson at Pfizer Global Research & Development for intellectual input and experimental assistance.

References

- Baillie, T.A., Pearson, P.G., 2000. The impact of drug metabolism in contemporary drug discovery: new opportunities and challenges for mass spectrometry. In: Burlingame, A.L., Carr, S.A., Baldwin, M.A. (Eds.), *Mass Spectrometry in Biology & Medicine* Humana Press, Totowa, NJ, pp. 481–496.
- Bakhtiar, R., Ramos, L., Tse, F.L.S., 2002. High-throughput mass spectrometric analysis of xenobiotics in biological fluids. *J. Liq. Chrom. Rel. Technol.* 25, 507–540.
- Berger, J., Moller, D.E., 2002. The mechanism of action of PPARs. *Annu. Rev. Med.* 53, 409–435.
- Borchardt, R.T., Freidinger, R.M., Sawyer, T.K., Smith, P.L., 1998. *Integration of Pharmaceutical Discovery and Development: Case Histories*. Plenum Press, New York, NY.
- Brewer, E., Henion, J., 1998. Atmospheric pressure ionization LC/MS/MS techniques for drug disposition studies. *J. Pharm. Sci.* 87, 395–402.
- Burton, K.I., Everett, J.R., Newman, M.J., Pullen, F.S., Richards, D.S., Swanson, A.G., 1997. On-line liquid chromatography coupled with high field NMR and mass spectrometry: a new technique for drug metabolite structure elucidation. *J. Pharm. Biomed. Anal.* 15, 1903–1912.
- Clayton, E., Taylor, S., Wright, B., Wilson, I.D., 1998. The application of high performance liquid chromatography, coupled to nuclear magnetic resonance spectroscopy and mass spectrometry (HPLC–NMR–MS), to the characterisation of ibuprofen metabolites from human urine. *Chromatographia* 47, 264–270.
- Cox, K.A., White, R.E., Korfmacher, W.A., 2002. Rapid determination of pharmacokinetic properties of new chemical entities: *in vivo* approaches. *Comb. Chem. High Throughput Screen* 5, 29–37.
- Dalvie, D.K., O'Donnell, J.P., 1998. Characterization of polar urinary metabolites by ionspray tandem mass spectrometry following dansylation. *Rapid Commun. Mass Spectrom.* 12, 419–422.

- Dear, G.J., Ayrton, J., Plumb, R., Fraser, I.J., 1999. The rapid identification of drug metabolites using capillary liquid chromatography coupled to an ion trap mass spectrometer. *Rapid Commun. Mass Spectrom.* 13, 456–463.
- Desai, R.C., Gratale, D.F., Han, W., Koyama, H., Metzger, E., Lombardo, V.K., MacNaul, K.L., Doebber, T.W., Berger, J.B., Leung, K., Franklin, R., Moller, D.E., Heck, J.V., Sahoo, S.P., 2003. Aryloxazolidinediones: identification of potent orally active PPAR dual α/γ agonists. *Bioorg. Med. Chem. Lett.* 13, 3541–3544.
- Eddershaw, P.J., Dickins, M., 1999. Advances in in vitro drug metabolism screening. *Pharm. Sci. Technol. Today* 2(1), 13–19.
- Hop, C.E.C.A., Yu, S., Xu, X., Singh, R., Wong, B., 2001. Elucidation of fragmentation mechanisms involving transfer of three hydrogen atoms using a quadrupole time-of-flight mass spectrometer. *J. Mass Spectrom.* 36, 575–579.
- Hop, C.E.C.A., Wang, Y., Kumar, S., Silva Elipe, M.V., Raab, C.E., Dean, D.C., Poon, G.K., Keohane, C.-A., Strauss, J., Chiu, S.-H.L., Curtis, N., Elliott, J., Gerhard, U., Locker, K., Morrison, D., Mortishire-Smith, R., Thomas, S., Watt, A.P., Evans, D.C., 2002. Identification of metabolites of a substance P (neurokinin 1 receptor) antagonist in rat hepatocytes and rat plasma. *Drug Metab. Dispos.* 30, 937–943.
- Hopfgartner, G., Chernushevich, I.V., Covey, T., Plomley, J.B., Bonner, R., 1999. Exact mass measurement of product ions for the structural elucidation of drug metabolites with a tandem quadrupole orthogonal-acceleration time-of-flight mass spectrometer. *J. Am. Soc. Mass Spectrom.* 10, 1305–1314.
- Hopfgartner, G., Bourgoigne, E., 2003. Quantitative high-throughput analysis of drugs in biological matrices by mass spectrometry. *Mass Spec. Rev.* 22, 195–214.
- Howard, H.R., Seeger, T.F., 1993. Novel antipsychotics. In: Bristol, J.A. (Ed.), *Annual Reports in Medicinal Chemistry*, Vol. 28. Academic Press, New York, NY, pp. 39–47.
- Howard, H.R., Prakash, C., Seeger, T.F., 1994. Ziprasidone hydrochloride. *Drugs of the Future* 19, 560–563.
- Johnson, K., Shah, A., Jaw, S., Baxter, J., Prakash, C., 2003. Metabolism, pharmacokinetics, and excretion of a highly selective NMDA receptor antagonist, traxoprodil, in human cytochrome P450 2D6 extensive and poor metabolizers. *Drug Metab. Dispos.* 31, 76–87.
- Knapp, D.R., 1979. *Handbook of Analytical Derivatization Reactions*. Wiley, New York, NY.
- Korfmacher, W.A., Cox, K.A., Bryant, M.S., Veals, J., Ng, K., Watkins, R., Lin, C.-C., 1997. HPLC-API/MS/MS: a powerful tool for integrating drug metabolism into the drug discovery process. *Drug Disc. Today* 2, 532–537.
- Kramer, M.S., Cutler, N., Feighner, J., Shrivastava, R., Carman, J., Sramak, J.J., Reines, S.A., Liu, G., Snavely, D., Wyatt-Knowles, E., Hale, J.J., Mills, S.G., MacCoss, M., Swain, C.J., Harrison, T., Hill, R.G., Hefti, F., Scolnick, E.M., Cascieri, M.A., Chicchi, G.G., Sadowski, S., Williams, A.R., Hewson, L., Smith, D., Carlson, E.J., Hargreaves, R.J., Rupniak, N.M.J., 1998. Distinct mechanism for antidepressant activity by blockade of central substance P receptors. *Science* 281, 1640–1645.
- Lee, M.S., Kerns, E.H., 1999. LC/MS applications in drug development. *Mass Spectrom. Rev.* 18, 187–279.

- Lee, M.S., 2002. LC/MS Applications in Drug Development. Wiley Interscience, New York, NY.
- Lim, H.K., Stellingweif, S., Sisenwine, S., Chan, K.W., 1999. Rapid drug metabolite profiling using fast liquid chromatography, automated multiple-stage mass spectrometry and receptor binding. *J. Chrom. A* 831, 227–241.
- Lin, J.H., Lu, A.Y.H., 1997. Role of pharmacokinetics and metabolism in drug discovery and development. *Pharmacol. Rev.* 49, 403–449.
- Liu, D.Q., Hop, C.E.C.A., Beconi, M.G., Mao, A., Chiu, S.-H.L., 2001. Use of on-line hydrogen/deuterium exchange to facilitate metabolite identification. *Rapid Commun. Mass Spectrom.* 15, 1832–1839.
- Louden, D., Handley, A., Taylor, S., Lenz, E., Miller, S., Wilson, I.D., Sage, A., 2000. Reversed-phase high-performance liquid chromatography combined with on-line UV diode array, FT infrared, and ^1H nuclear magnetic resonance spectroscopy and time-of-flight mass spectrometry: application to a mixture of nonsteroidal antiinflammatory drugs. *Anal. Chem.* 72, 3922–3926.
- Mayol, R.F., Jajoo, H.K., Klunk, J., Blair, I.A., 1991. Metabolism of the antipsychotic drug tiospirone in humans. *Drug Metab. Dispos.* 19, 394–399.
- Meltzer, H.Y., 1995. Role of serotonin in the action of atypical antipsychotic drugs. *Clin. Neurosci.* 3, 64–75.
- Moller, D.E., 2001. New drug targets for type 2 diabetes and the metabolic syndrome. *Nature* 414, 821–827.
- Navari, R.M., Reinhardt, R.R., Gralla, R.J., Kris, M.G., Hesketh, P.J., Khojasteh, A., Kindler, H., Grote, T.H., Pendergrass, K., Grunberg, S.M., Carides, A.D., Gertz, B.J., 1999. Reduction of cisplatin-induced emesis by a selective neurokinin-1-receptor antagonist. *N. Engl. J. Med.* 340, 190–195.
- Niessen, W.M.A., 1998. Advances in instrumentation in liquid-chromatography-mass spectrometry and related liquid-introduction techniques. *J. Chrom. A* 794, 407–435.
- Olsen, M.A., Cummings, P.G., Kennedy-Gabb, S., Wagner, B.M., Nicol, G.R., Munson, B., 2000. The use of deuterium oxide as a mobile phase for structural elucidation by HPLC/UV/ESI/MS. *Anal. Chem.* 72, 5070–5078.
- Ortiz, A., Gershon, S., 1986. The future of neuroleptic psychopharmacology. *J. Clin. Psychiatry* 47 (Suppl.), 3–11.
- Poon, G.K., 1997. Drug metabolism and pharmacokinetics. In: Cole, R.B. (Ed.), *Electrospray Ionization Mass Spectrometry: Fundamentals, Instrumentation & Applications*. Wiley, New York, NY, pp. 499–525.
- Prakash, C., Kamel, A., Anderson, W., Howard, H., 1997. Metabolism and excretion of the antipsychotic drug ziprasidone in rat following oral administration of a mixture of ^{14}C - and ^3H -labeled ziprasidone. *Drug Metab. Dispos.* 25, 206–218.
- Prakash, C., Soliman, V., 1997. Metabolism and excretion of a novel antianxiety drug candidate, CP-93,393 in Long Evans rats: differentiation of regioisomeric glucuronides by LC/MS/MS and LC/MS/MS/MS. *Drug Metab. Dispos.* 25, 1288–1297.
- Prakash, C., Cui, D., 1997. Metabolism and excretion of a new antianxiety drug candidate, CP-93,393, in cynomolgus monkeys. *Drug Metab. Dispos.* 25, 1395–1406.

- Qin, X., Frech, P., 2001. Liquid chromatography/mass spectrometry (LC/MS) identification of photooxidative degradates of crystalline and amorphous MK-912. *J. Pharm. Sci.* 90, 833–844.
- Riley, R.J., Martin, I.J., Cooper, A.E., 2002. The influence of DMPK as an integrated partner in modern drug discovery. *Curr. Drug Metab.* 3, 527–550.
- Rodriguez, R.J., Proteau, J.P., Marquez, B.L., Hetherington, C.L., Buckholz, C.J., O'Connell, K.L., 1999. Flavin-containing monooxygenase-mediated metabolism of *N*-deacetyl ketoconazole by rat hepatic microsomes. *Drug Metab. Dispos.* 27, 880–886.
- Rollema, H., Clarke, T., Lu, Y., Schmidt, A.W., Sprouse, J.S., 1996. Comparison of the effects of CP-93,393 and buspirone on 5HT and NE release: microdialysis studies in the hippocampus of freely moving rat and guinea pig. *J. Neurochem.* 66 (Suppl. 2), S37.
- Rossi, D.T., Sinz, M.W., 2002. *Mass Spectrometry in Drug Discovery*. Marcel Dekker, Inc., New York, NY.
- Rushmore, T.H., Reider, P.J., Slaughter, D., Assang, C., Shou, M., 2000. Bioreactor systems in drug metabolism: synthesis of cytochrome P450-generated metabolites. *Metab. Eng.* 2, 115–125.
- Schmidt, A.W., Fox, C.B., Lazzaro, J., McLean, S., Ganong, A., Schulz, D.W., Desai, K., Bright, G.M., Heym, J., 1995. CP-93,393, a novel anxiolytic-antidepressant agent with both 5-HT_{1A} agonist and alpha-2 adrenergic properties: in vitro studies. *Neurosci. Abstr.* 21, 2106.
- Shockcor, J.P., Unger, S., Wilson, I.D., Foxall, P.J.D., Nicholson, J.K., Lindon, J.C., 1996. Combined HPLC, NMR spectroscopy, and ion-trap mass spectrometry with application to the detection and characterization of xenobiotic and endogenous metabolites in human urine. *Anal. Chem.* 68, 4431–4435.
- Smith, D., Schmid, E., Jones, B., 2002. Do drug metabolism and pharmacokinetic departments make any contribution to drug discovery. *Clin. Pharmacokinet.* 41, 1005–1019.
- Tarsey, D., 1983. Neuroleptic-induced extrapyramidal reactions: classification, description, and diagnosis. *Clin. Neuropharmacol.* 6 (Suppl. 1), S9–S26.
- Tattersall, F.D., Rycroft, W., Cumberbatch, M., Mason, G., Tye, S., Williamson, D.J., Hale, J.J., Mills, S.G., Finke, P.E., MacCoss, M., Sadowski, S., Ber, E., Cascieri, M., Hill, R.G., MacIntyre, D.E., Hargreaves, R.J., 2000. The novel NK1 receptor antagonist MK-0869 (L-754,030) and its water soluble prodrug, L-758,298, inhibit acute and delayed cisplatin-induced emesis in ferrets. *Neuropharmacology* 39, 652–663.
- Tiller, P.R., Land, A.D., Jardine, I., Murphy, D.M., Sozio, R., Ayrton, A., Schaefer, W.H., 1998. Application of liquid chromatography–mass spectrometryⁿ analyses to the characterization of novel glyburide metabolites formed in vitro. *J. Chrom. A* 794, 15–25.
- Tiller, P.R., Raab, C., Hop, C.E.C.A., 2001. An unusual fragmentation mechanism involving the transfer of a methyl group. *J. Mass Spectrom.* 36, 344–345.
- White, R.E., 2000. High-throughput screening in drug metabolism and pharmacokinetic support of drug discovery. *Annu. Rev. Pharmacol. Toxicol.* 40, 133–157.

- Wienkers, L.C., Steenwyk, R.C., Mizesak, S.A., Pearson, P.G., 1995. In vitro metabolism of tirilazad mesylate in male and female rats. *Drug Metab. Dispos.* 23, 383–392.
- Wienkers, L.C., Steenwyk, R.C., Sanders, P.E., Pearson, P.G., 1996. Biotransformation of tirilazad in human: 1. cytochrome P450 3A-mediated hydroxylation of tirilazad mesylate in human liver microsomes. *J. Pharmacol. Exp. Ther.* 277, 982–990.
- Willoughby, R., Sheehan, E., Mitrovich, S., 1998. *A Global View of LC/MS: How to Solve Your Most Challenging Analytical Problems*. Global View Publishing, Pittsburgh, PA.
- Woolf, T.F., 1999. *Handbook of Drug Metabolism*. Marcel Dekker, Inc., New York, NY.
- Yu, X., Cui, D., Davis, M.R., 1999. Identification of in vitro metabolites of indinavir by “Intelligent Automated LC–MS/MS” (INTAMS) utilizing triple quadrupole tandem mass spectrometry. *J. Am. Soc. Mass Spectrom.* 10, 175–183 and references therein.
- Zimmet, P., Alberti, K.G.M.M., Shaw, J., 2001. Global and societal implications of the diabetes epidemic. *Nature* 414, 782–787.